The evolution of a Na^+-sensitive *Vibrio cholerae* mutant unmasks the moonlighting aminopeptidase PepA as a regulator of *nhaB* Na^+/H^+ antiporter gene expression

Sebastian Herdan[1§], Katharina Kohm[2§], Robert Warneke[3], Florian Roth[2], Nicolas Görge[1], Trung Duc Hoang[4], Emina Schunke[1], Claudia C. Häse[5], Juri Rappsilber[3], Günter Fritz[1], Fabian M. Commichau[2], Johannes Gibhardt[4], Julia Steuber[1]

[1]FG Cellular Microbiology 190 i, Institute for Biology, University of Hohenheim, Stuttgart, Germany
[2]FG Molecular Microbiology 190 h, Institute for Biology, University of Hohenheim, Stuttgart, Germany
[3]FG Bioanalytics, Technical University of Berlin, Germany
[4]FG Microbial Processes of Nitrogen Transformation 190 y, Institute for Biology, University of Hohenheim, Stuttgart, Germany
[5]Carlson College of Veterinary Medicine, Oregon State University, Corvallis, Oregon, USA

[&]The authors should be regarded as joint first authors

ABSTRACT

The pathogenic bacterium *Vibrio cholerae* is native to seawater and can therefore be cultivated in nutrient media with increased salt concentration. To maintain osmotic balance, *V. cholerae* uses Na^+/H^+ antiporters and an Na^+-translocating NADH:quinone oxidoreductase (Na^+-NQR). The exact contribution of the various Na^+/H^+ antiporters to maintain Na^+ and H^+ homeostasis in *V. cholerae* is unclear. However, genetic studies indicate the major Na^+/H^+ antiporter NhaA and the Na^+-NQR are required by the bacteria for Na^+ resistance at alkaline conditions. Here we show that the growth defect of a *V. cholerae nhaA nqr* mutant at increased Na^+ concentrations and alkaline pH is relieved by the rapid acquisition of suppressor mutations. The suppressor mutants could be assigned to two classes. We identified (i) mutations in the promoter of the *nhaB* gene encoding a Na^+/H^+ antiporter and (ii) mutations that either affect the expression level of the *pepA* gene or DNA binding activity of the encoded multifunctional aminopeptidase PepA. The characterization of the P_{nhaB} and P_{pepA} promoters of the suppressor mutants, membrane potential measurements and comparative proteome analyses identified PepA as a novel factor controlling Na^+ homeostasis in *V. cholerae.*

41 **IMPORTANCE**

42 The emergence and spread of multi-resistant bacteria are a major problem for humans and
43 animals. Therefore, the identification of novel targets for the development of novel antibiotics
44 to combat pathogenic bacteria is extremely important. Since sodium ion homeostasis is an
45 essential process in many pathogenic bacteria, especially those living in marine environments,
46 it represents an interesting target for antibiotics. The perturbation of sodium ion homeostasis
47 does indeed impair the fitness of the human pathogenic bacterium *Vibrio cholerae* but can be
48 restored by the rapid evolution of the bacteria. This suggests that inhibiting multiple targets
49 with different antibiotics might be more effective in preventing the development of resistant
50 bacteria.

51

52 **INTRODUCTION**

53 To maintain osmotic balance, all living cells must be capable of extruding sodium ions (Na^+)
54 from the cytoplasm to the extracellular space. Moreover, bacteria like alkaliphilic *Bacilli* and
55 marine *Vibrio* use Na^+-driven flagellar motor complexes for locomotion in their aquatic habitats
56 [1]. To prevent the accumulation of Na^+, these bacteria rely on transport systems for the export
57 of the cation. The extrusion of Na^+ can be achieved with the help of Na^+/H^+ antiporters, which
58 are secondary transporters that couple the export of Na^+ to the import of H^+ [2-8]. For instance,
59 in *Escherichia coli*, the export of Na^+ is driven by at least two distinct Na^+/H^+ antiporters, NhaA
60 and NhaB, of which the former is required for the maintenance of the cytoplasmatic pH at
61 alkaline pH [9-13]. The expression of the *nhaA* gene is positively controlled by the LysR-type
62 DNA-binding transcription factor NhaR that responds to Na^+ [14-17]. NhaA couples the export
63 of 2 Na^+ to the import of 3 H^+ and therefore is crucial for acidification of the cytoplasm under
64 alkaline conditions [18]. Moreover, some bacteria can establish an electrochemical sodium
65 gradient using primary Na^+ pumps, such as the Na^+-translocating NADH:quinone
66 oxidoreductase (Na^+-NQR) [19], or the Na^+-pumping oxaloacetate decarboxylase [20]. The
67 Na^+-NQR is a six-subunit, respiratory complex that couples the oxidation of NADH and
68 reduction of ubiquinone to the translocation of Na^+ across the inner bacterial membrane [21].

69 In *Vibrio cholerae*, the causative agent of Cholera disease, the Na^+-NQR operates together
70 with several Na^+/H^+ antiporters [6,22] to ensure survival in very different habitats, ranging from
71 alkaline marine environment with high salinity to acidic compartments in the human
72 gastrointestinal tract [23,24]. Moreover, virulence and pathogenicity of *V. cholerae* are
73 intimately linked to the activity of the Na^+-NQR [23,25], marking the protein complex and other
74 respiratory enzymes of pathogenic bacteria as putative drug targets [26,27].

75 In addition to the Na^+-NQR, five antiporter systems have been identified in *V. cholerae*
76 that contribute to Na^+ and H^+ homeostasis [19]. For instance, the Na^+/H^+ antiporter NhaA in *V.*
77 *cholerae* [28], is the homolog of NhaA from *E. coli* [29]. Like in *E. coli*, the expression of the
78 *nhaA* gene depends on the Na^+-responsive transcriptional activator NhaR [30]. Moreover,
79 NhaB, of which also a homolog exists in *E. coli*, is a Na^+/H^+ antiporter that confers resistance
80 to Na^+ and Li^+ when overproduced in an *E. coli nhaA nhaB* mutant [6,31]. The $K^+(Na^+)/H^+$
81 antiporter NhaP1 also seems to be required for pH homeostasis in *V. cholerae* [32].
82 Furthermore, the multi-subunit Na^+/H^+ antiporter Mrp allowed the *E. coli nhaA nhaB* mutant to
83 grow at toxic Na^+ and Li^+ concentrations as well as with natural bile salts [33]. While the exact
84 contribution of the Na^+/H^+ antiporters NhaB, NhaD, NhaP1 and Mrp in maintaining Na^+ and H^+
85 homeostasis in *V. cholerae* is yet unclear, NhaA can be considered as the major Na^+/H^+
86 antiporter that, together with the Na^+-NQR, was shown to be required by the bacteria for Na^+
87 resistance at alkaline conditions [6].

88 In the present study, we confirmed that the *nhaA* and *nqr* genes encoding the Na^+/H^+
89 antiporter NhaA and Na^+-NQR, respectively, become synthetically lethal in *V. cholerae* at high
90 Na^+ concentrations and pH. Serendipitously, we found that the *V. cholerae nhaA nqr* mutant
91 is genomically highly unstable and rapidly forms suppressor mutants in which Na^+/H^+
92 homeostasis is restored. The characterization of the suppressor mutants revealed that
93 restoration of Na^+/H^+ homeostasis can be achieved by the strong overexpression of the *nhaB*
94 Na^+/H^+ antiporter gene. The suppressor screen also identified the multifunctional PepA protein
95 as a novel repressor of the *nhaB* gene because loss-of-function mutations in *pepA* results in
96 NhaB overproduction and Na^+ resistance. As an aminopeptidase, PepA is involved in amino

97 acid metabolism, and the protein's DNA binding activity controls plasmid segregation and gene
98 expression. The role of PepA in maintaining Na^+/H^+ homeostasis in *V. cholerae* is discussed.
99
100 **RESULTS**
101 **Genomic stability of a *V. cholerae nqr nhaA* mutant at high salinity and alkaline pH**
102 Previously it was observed that the mutational inactivation of the *nhaA*, *nhaB* and *nhaD* Na^+/H^+
103 antiporter genes in *V. cholerae* did not affect exponential growth of the bacteria [6]. Moreover,
104 a *V. cholerae nqr* mutant lacking the NQR complex did not show defects in Na^+-pumping-
105 related phenotypes [34]. This suggests that other secondary Na^+ pumps can compensate for
106 the lack of NQR. Indeed, the selective inhibition of the NQR by 2-*n*-nonyl-4-hydroxyquinoline
107 *N*-oxide uncovered that the NhaA Na^+/H^+ antiporter becomes essential for Na^+ resistance at
108 alkaline conditions [6]. Since the NQR is an interesting target for novel antibiotics, we assessed
109 the genomic stability of a *V. cholerae* strain lacking the major Na^+/H^+ antiporter and the primary
110 pump. For this purpose, we cultivated the wild type, the *nhaA* and *nqr* single mutants, and the
111 *nhaA nqr* double mutant in standard LB medium (pH 6.2, 171 mM NaCl) or in LB with Tris-
112 buffered pH (pH 7.8) without additional NaCl (residual Na^+ concentration, 13 mM). As shown
113 in **Figures 1A** and **1B**, the strains lacking the NQR produced slightly less biomass during
114 stationary growth phase. This indicates some contribution to Na^+ extrusion by the primary Na^+
115 pump under these conditions. In contrast, *nhaA nqr* mutant showed a severe growth defect in
116 alkaline LB medium containing 150 mM NaCl (**Figure 1C**). As expected, the growth defect of
117 the *nhaA nqr* mutant can be relieved by plasmid-based overexpression of the *nqr* operon
118 (**Figure 1D**). Thus, in perfect agreement with earlier studies, the *nhaA* and *nqr* genes are
119 synthetically lethal in *V. cholerae* at high salinity and alkaline pH [6,35]. However, after 17 h of
120 growth a transition to almost wild type growth rate was observed for the *nhaA nqr* mutant
121 (**Figure 1C**). This indicates that this mutant is genomically unstable and theresulting selective
122 pressure leads to rapid emergence of suppressor mutations that confer Na^+ resistance.
123

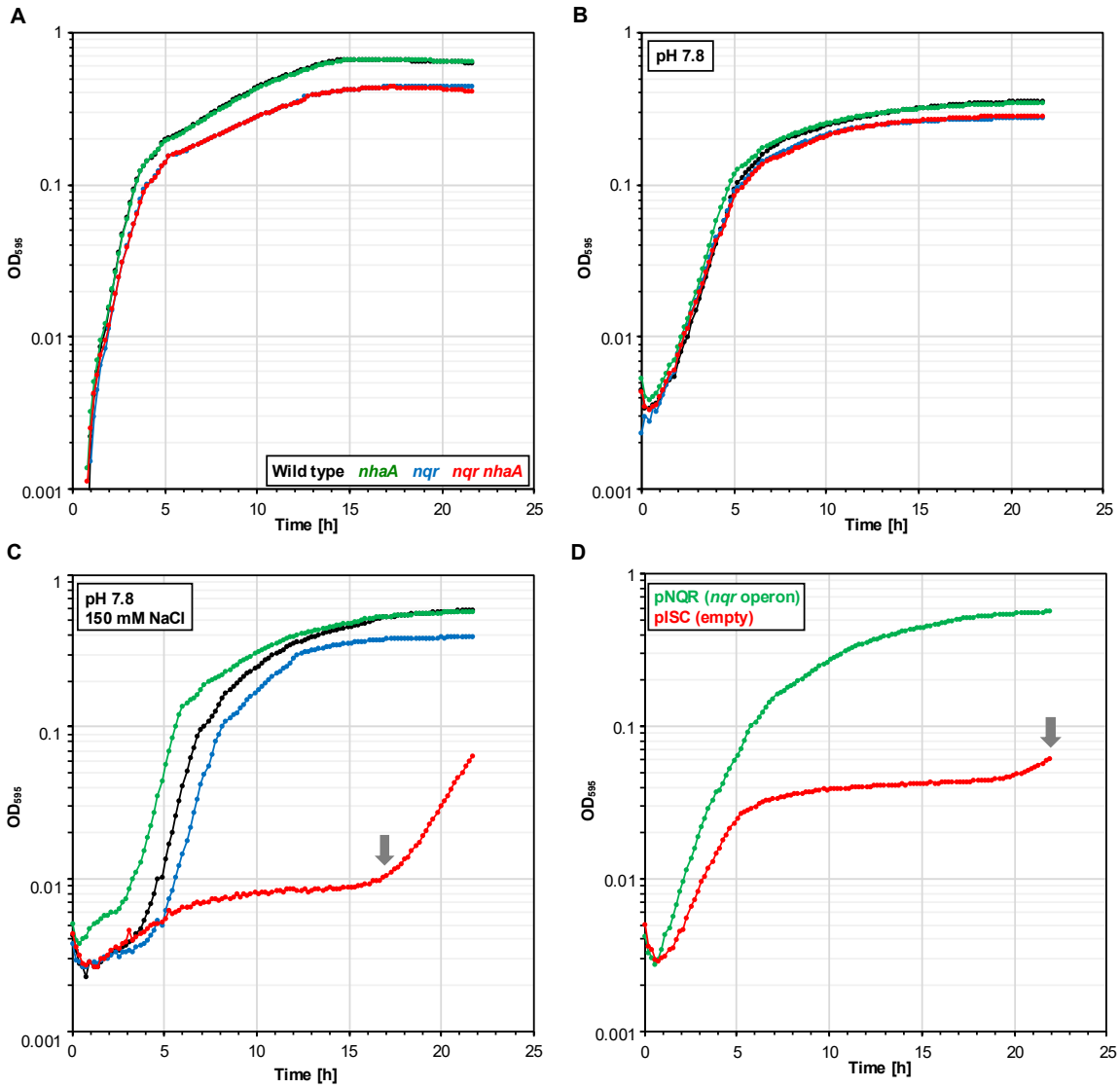

Figure 1 - Influence of salinity and pH on growth of *V. cholerae* mutants with impaired Na^+ export. Growth of the wild type and the *nhaA*, *nqr* and *nqr nhaA* mutants in LB medium (pH 6.2, 171 mM NaCl) (**A**), in LB_{Tris} (pH 7.8, 13 mM Na^+) (**B**), and in LB_{Tris} (pH 7.8) in the presence of 150 mM NaCl (**C**). Growth of the *nqr nhaA* mutant carrying the empty plasmid pISC or the plasmid pNQR for the overexpression of the NQR in LB_{Tris} medium at pH 7.8 in the presence of 150 mM NaCl (**D**). The cultivation experiments were carried out in a multi-well plate reader at 30 °C. The grey arrows indicate the emergence of suppressor mutants.

Characterization of *V. cholerae nqr nhaA* suppressor mutants

We repeatedly observed that the *V. cholerae nqr nhaA* mutant when grown in LB medium at high salinity and pH 7.8 resumed growth (**Figures 1C** and **1D**; data not shown). As described above, this indicates the formation of Na^+-resistant suppressor mutants that probably overproduce a Na^+ extrusion system. To understand the underlying molecular mechanism of Na^+ homeostasis restoration in the background of the *V. cholerae nqr nhaA* mutant, we isolated suppressor mutants. For this purpose, we grew the mutant overnight in standard LB medium

140 (pH 6.1, 171 mM NaCl), washed the cells twice in standard LB and propagated the bacteria
141 on selective LB plates (pH 7.8, 150 mM NaCl). After incubation for 5 days at 30°C,
142 approximately 250 suppressor mutants appeared on the plates on which 10^7 cells had been
143 distributed (**Figure 2A**). Next, we isolated 20 independent suppressors (S1 – S20) (Table 1)
144 and verified the genetic stability of the mutants by passaging of the bacteria on standard LB
145 plates and subsequent selection at high salinity and alkaline pH. The cultivation of a selected
146 set of mutants (S3, S4 and S7) in selective LB medium confirmed their Na^+ resistance. As
147 shown in **Figure 2A**, even though the mutants produced less biomass, their growth rates were
148 comparable to that of the wild type strain. The determination of the membrane potential (**Figure**
149 **2B**) revealed that all mutants were less impaired in formation of membrane potential than the
150 parental *V. cholerae nqr nhaA* strain. Furthermore, potentials of the mutants were at least as
151 high as the ones of the *V. cholerae nqr* strain, thus resembling rescue from the *nhaA* deletion
152 in the parental strain. To conclude, the *V. cholerae nqr nhaA* mutant is genetically unstable
153 and quickly adapts to high salinity and alkaline pH through the accumulation of beneficial
154 mutations.
155
156
157
158
159
160
161
162
163
164
165
166
167
168
169
170
171
172
173

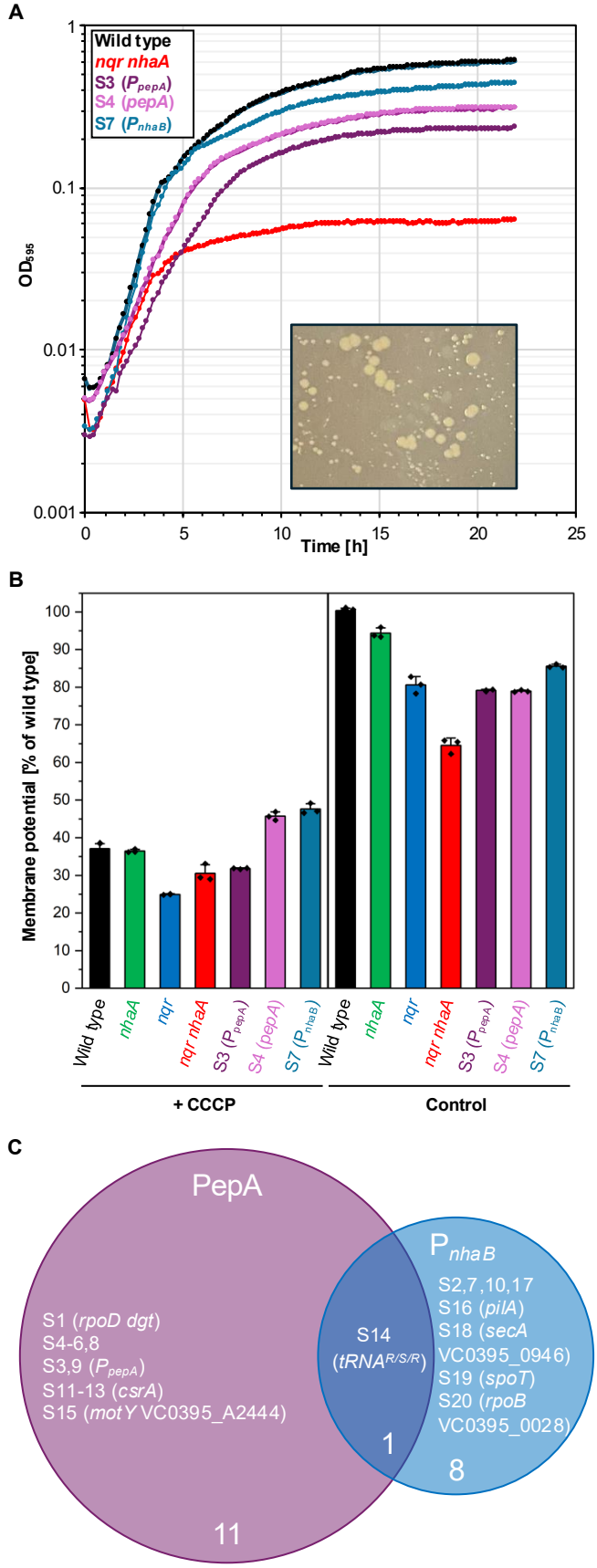

Figure 2. Characterisation of selected suppressor mutants and identified genomic alterations relieving the growth defect of the *nqr nhaA* mutant. (**A**) Growth of the wild type, the *nhaA*, *nqr* mutant, and the suppressor mutants S3, S4 and S7 in LB medium at pH 7.8 in the presence of 150 mM NaCl. The cultivation experiments were carried out in a multi-well plate reader at 30 °C. The Figure inlay shows the suppressor mutants that emerged during growth under selection. (**B**) Determination of the membrane potential in the wild type, the *nhaA*, mutant, the *nqr* mutant, the *nhaA*, *nqr* mutant, and the suppressor mutants S3, S4 and S7. (**C**) Venn diagram illustrating the overlap of the genomic regions mutated in the *nqr nhaA* strain during growth under selection (see also Table 1).

211

212

213 **Identification of the mutations in the *nqr nhaA* suppressors**

214 Genome sequencing of the 20 isolated suppressors allowed us to assign the mutants to two
215 different classes. Nine mutants had acquired a mutation in a genomic region that likely contains
216 the promoters of the *nhaB* and *fadR* genes (**Figure 2C** and **3A**). The *fadR* gene encodes a
217 DNA-binding transcription factor that is involved in fatty acid degradation and biosynthesis
218 [36,37]. Since NhaB is a Na^+/H^+ antiporter, the mutations in the *fadR-nhaB* intergenic region
219 likely increase the activity of the P_{nhaB} promoter, which result in overproduction of NhaB and
220 thus Na^+ resistance of the *V. cholerae nqr nhaA* suppressors. Interestingly, three P_{nhaB}
221 promoter variants emerged independently of each other twice (**Figure 3A**) (Table 1). The
222 remaining 12 suppressor mutants all had acquired mutations that either affect the expression
223 levels of the *lptF* and *pepA* genes, or the coding sequence of the *pepA* gene (**Figure 2C, 4A**)
224 (Table 1). The suppressor S14 with a mutation in the *pepA* gene also had deleted a 27 bp-
225 long sequence in the *fadR-nhaB* intergenic region. Recently, chromatin immuno precipitation
226 sequencing (ChIP-Seq) experiments revealed that PepA is a global transcription repressor in
227 *V. cholerae* [38]. Interestingly, the *fadR-nhaB* and *lptF-pepA* intergenic regions were also
228 identified as PepA binding sites (**Figure 3A, Figure S2**). This suggests that the mutations in
229 the *fadR-nhaB* and *lptF-pepA* intergenic regions may abolish the PepA-dependent repression
230 of the P_{nhaB} promoter and affect negative autoregulation and thus the cellular concentration of
231 the repressor.

232 As with the first class of mutants, two *pepA* mutations were also identified multiple times
233 (Table 1). Moreover, five *pepA* mutants had acquired additional mutations in genes whose
234 coding products are involved in post-transcriptional regulation (CsrA), Na^+-driven motility
235 (MotY), cell surface structure (PilA), stringent response (SpoT), information processing (Dgt,
236 RpoB, RpoD), and protein secretion (SecA), translation ($tRNA^{Arg}$ $tRNA^{Ser}$), and unknown
237 processes (VC0395_0946, VC0395_A2444) [39-42]. However, the fact that in six mutants of
238 the second large group of suppressors only the *pepA* gene or the *lptF-pepA* intergenic region
239 were altered suggests that the encoded protein is involved in the control of Na^+ extrusion in *V.*
240 *cholerae*. In summary, the link between PepA and Na^+ resistance in the *nqr nhaA* suppressors

241 appears less obvious at first glance. However, it is often the case that different mutations

242 produce similiar phenotypes in suppressor screens [43-45].

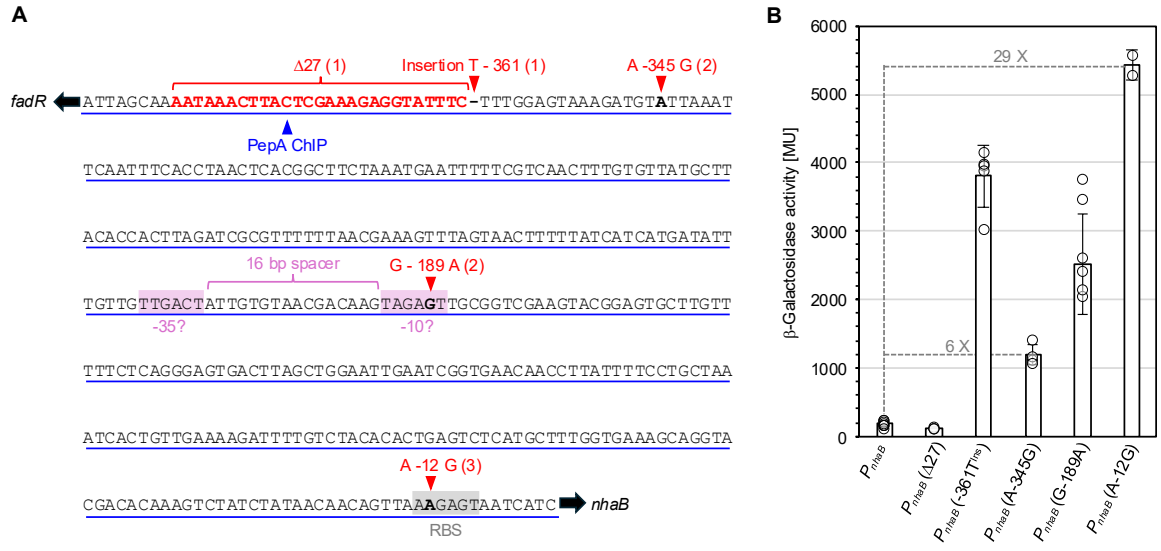

243

244 **Figure 3. Characterization of the P_{nhaB} promoter variants of the *nqr nhaA* suppressors.**
245 (**A**) *fadR-nhaB* intergenic region located on chromosome 1 of *V. cholerae.* The identified
246 mutations are indicated in red and are specified in relation to the start codon of the *nhaB* gene.
247 The PepA binding site in the P_{nhaB} promoter is underlined and the region that was most
248 enriched in the ChIP-Seq experiment (14-fold) is indicated by a blue arrow [38]. RBS,
249 ribosome-binding site. A possible promoter created or improved by the mutation A -189 A
250 mutation is highlighted in pink. (**B**) β-Galactosidase assay to assess the effect of the mutations
251 in the *fadR-nhaB* intergenic region on the activity of the P_{nhaB} promoter in *E. coli* XL1-Blue. The
252 cells were grown in LB medium at 37 °C and harvested at an OD_{600} between 0.5 and 0.8. β-
253 Galactosidase activities are given as units per milligram protein. Experiments were carried out
254 at least three-fold. Mean values are indicated by columns.
255

256 ***nhaB* overexpression restores the growth defect of the *nqr nhaA* mutant**

257 To assess whether the mutations in the *fadR-nhaB* intergenic region of the *V. cholerae nqr*

258 *nhaA* suppressors affect the activity of the P_{nhaB} promoter, we constructed translational *nhaB-*

259 *lacZ* fusions and introduced the plasmids into *E. coli* XL1-Blue. Unfortunately, a *lacZ*-based

260 reporter system to assess the activity of the P_{nhaB} promoter could not be used in our *V. cholerae*

261 strain because it already contains a *lacZ* gene in the *toxT* locus (Table 1). However, since

262 *E. coli* and *V. cholerae* are both γ-proteobacteria, we assumed that the wild type P_{nhaB} promoter

263 and the mutant derivatives must also be active in *E. coli*. It has indeed been shown that a *V.*

264 *cholerae* DNA-binding regulator can replace the functional homolog in *E. coli* [30]. Next, the

265 strains were grown in LB medium, and the cells were harvested during mid-exponential growth

266 (OD_{600} 0.5 – 0.8). Except for the promoter with the 27 bp-long deletion (derived from

267 suppressor S14), all promoters with single nucleotide exchanges were 6 – 29-fold more active
268 than the wild type P_{nhaB} promoter (**Figure 3B**). In suppressor S14, the mutation in *pepA* likely
269 causes de-repression of the P_{nhaB} promoter in *V. cholerae* (see below). To conclude, it is
270 reasonable to assume that, due to the mutations in the *fadR-nhaB* intergenic region, the *V.*
271 *cholerae nqr nhaA* suppressors overproduce Na^+/H^+ antiporter NhaB, which leads to Na^+
272 resistance through increased export of the cation.
273

274 **A potential link between DNA-binding activity of PepA and *nhaB* gene expression**

275 The remaining 12 *nqr nhaA* suppressor mutants all had acquired mutations that either affect
276 the expression level or the coding sequence of the *pepA* gene (**Figure 2C**) (Table 1). In two
277 suppressors (S3 and S9), the same nucleotide was deleted in the *lptF-pepA* intergenic region
278 (**Figure 4A**). While *lptF* codes for an essential component of a lipopolysaccharide transport
279 system, the *pepA* aminopeptidase gene is not essential in *V. cholerae* [38,46]. Therefore, it is
280 unlikely that the mutation in the suppressors S3 and S9 would affect *lptF* expression. To
281 assess the wild type and mutant P_{lptF} and P_{pepA} promoters, we constructed translational *lptF-*
282 and *pepA-lacZ* fusions and introduced the plasmids into *E. coli* XL1-Blue. Next, we propagated
283 the transformants on LB plates containing X-Gal. The *E. coli* cells carrying the wild type and
284 mutated *lptF-lacZ* fusions both formed dark blue colonies. The β-galactosidase assay
285 confirmed that the mutation in the *lptF-pepA* intergenic region does not affect the activity of the
286 P_{lptF} promoter (**Figure 4B, 4C**). In contrast, cells with the mutated *pepA-lacZ* fusion formed
287 white colonies on the plates compared to the cells with the wild type-promoter (**Figure 4B**).
288 This made it more difficult to identify positive clones using blue-white screening. The β-
289 galactosidase test revealed that the mutated *pepA-lacZ* fusion was about 17-fold less active
290 (**Figure 4C**). In summary, the mutation in the P_{pepA} promoter of the suppressors S3 and S9
291 likely leads to a reduction of the cellular PepA concentration. Using the *E. coli pepA* wild type
292 and *pepA::tet* strains, we tested whether *E. coli* PepA has an influence on the *nhaB-lacZ* fusion.
293 However, this was not the case (data not shown).

294 The remaining 10 suppressors carry mutations in *pepA* that likely affect the DNA-
295 binding activity of the encoded protein (**Figure 2C, 4D**) (Table 1). For instance, four
296 suppressors (S4, S5, S6 and S8) had acquired a stop codon that would truncate PepA by 228
297 or 347 amino acids (**Figure 4B**). An extensive characterization of PepA mutant variants from
298 *E. coli* revealed that the N-terminal domain (residues 1 – 166) is involved in DNA binding,
299 whereas the C-terminal domain (residues 193 – 503) that is connected by an α-helix (residues
300 167 – 192) is required for aminopeptidase activity (**Figure 4D, 4E**) [47,48]. Thus, the truncation
301 in S4 – S6 and S8 probably leads to a general defect in PepA folding or oligomerization and
302 thus to the loss of DNA-binding and aminopeptidase activities. The remaining six suppressors
303 contain *pepA* alleles that code for PepA variants with single amino acid exchanges, among
304 them four with replacements of arginine 164 (**Figure 4D, 4E**). The suppressor S15 synthesizes
305 a PepA variant in which a residue located near arginine 164 in PepA was replaced. The
306 arginine 164 was previously identified as crucial for the DNA-binding activity of *E. coli* PepA
307 [48]. Therefore, the exchange of arginine 164 and neighboring residues likely affects the DNA-
308 binding activity of *V. cholerae* PepA. The suppressor S1 synthesizes a PepA variant in which
309 aspartate 435 is replaced by tyrosine (**Figure 4D, 4E**). Even though the aminopeptidase
310 domain is altered in this PepA variant, changes in the C-terminal domain can lead to both
311 enzyme functions being impaired [48]. As described above, PepA is a global transcription
312 factor that has many chromosomal binding sites, including the P_{nhaB} and P_{pepA} promoters
313 (**Figure 3A, 4A**) [38]. Moreover, suppressor S14 had deleted a part of the PepA binding site
314 in the P_{nhaB} promoter and synthesizes a PepA variant in which the arginine 164 is replaced by
315 leucine (**Figure 3A, 4D, 4E**). Thus, the synthesis of the PepA R164L variant and the deletion
316 of the PepA binding site in the P_{nhaB} promoter likely have a synergistic effect on *nhaB*
317 expression in *V. cholerae*. In summary, the suppressor analysis suggests that PepA is involved
318 in Na^+ homeostasis by controlling the expression of the *nhaB* Na^+/H^+ antiporter gene.

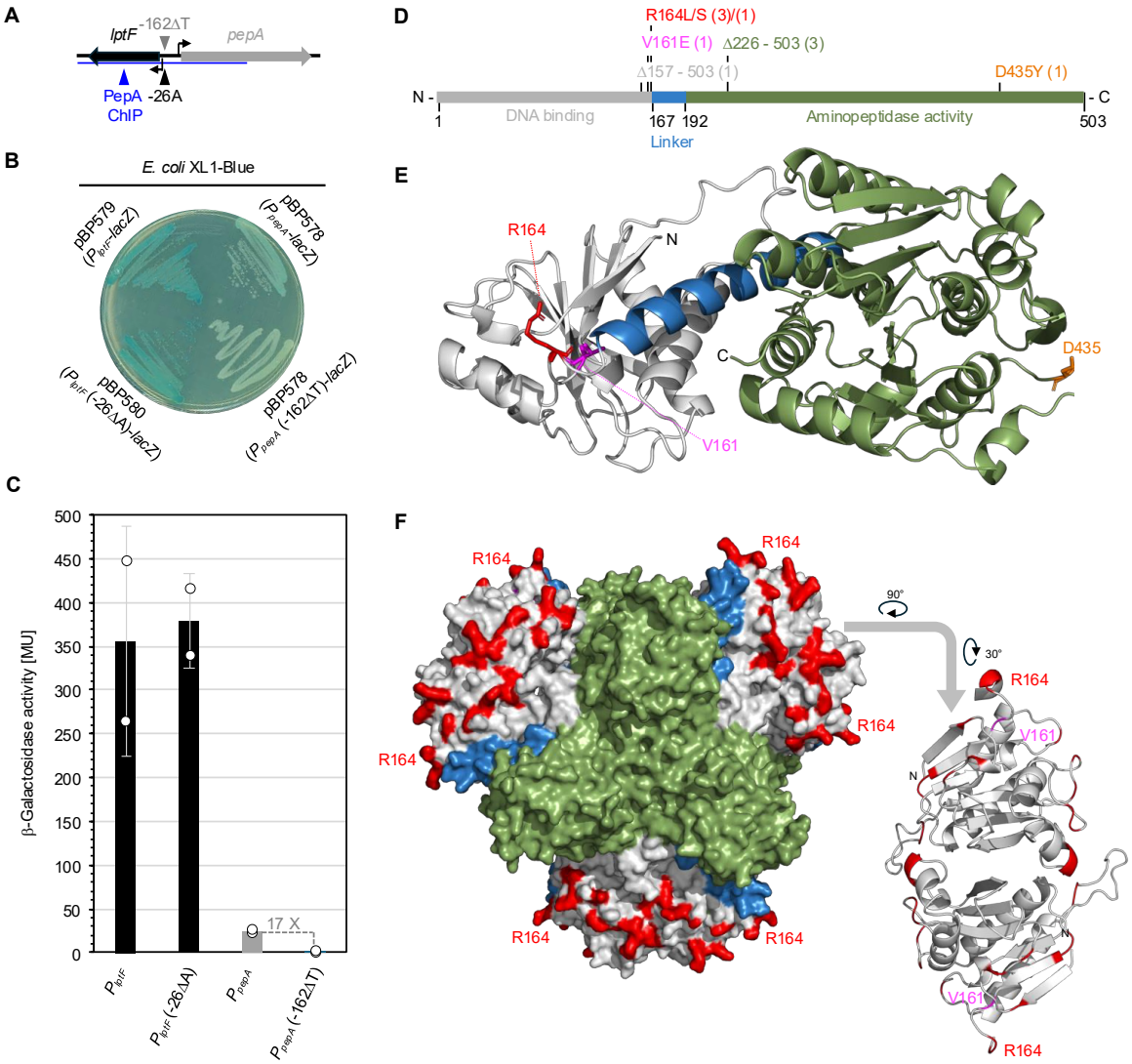

Figure 4. Characterization of the P_{pepA} promoter variant and PepA variants in the *nqr nhaA* suppressors. (**A**) *lptF-pepA* intergenic region located on chromosome 1 of *V. cholerae.* The identified mutation is specified in relation to the start codons of the genes. The PepA binding site in the *lptF-pepA* intergenic region is underlined and the region that was most enriched in the ChIP-Seq experiment is indicated by a blue arrow [38] (**B**) Qualitative test to visualize the activities of the P_{pepA} and P_{lptF} promoters in *E. coli* XL1-Blue that was propagated on LB medium containing the chromogenic substrate X-Gal. The plates were incubated for 24 h at 37 °C. (**C**) β-Galactosidase assay to assess the effect of the mutation in the *lptF-pepA* intergenic region on the activity of the P_{pepA} and P_{lptF} promoters in *E. coli* XL1-Blue. The cells were grown in LB medium at 37 °C and harvested at an OD_{600} between 0.5 and 0.8. β-Galactosidase activities are given as units per milligram protein. Experiments were carried out at least three-fold. Mean values are indicated by columns. (**D**) Amino acid replacements in PepA. The numbers in parentheses indicate how often the PepA variants were identified. (**C**) Localization of the amino acid exchanges in a full-length PepA model based on the structure of the *E. coli* homolog (PDBid: 1GYT). (**F**) Molecular surface of the *V. cholerae* PepA hexamer. The amino acid residues that were previously identified to be important for DNA-binding activity and XerCD-dependent recombination are labelled in red [48].

340 **Identification of PepA in the *nqr nhaA* suppressors and PepA-regulated genes**

341 To evaluate how the reduced PepA synthesis, the synthesis of a truncated PepA variant, or
342 the increased P_{nhaB} promoter activity affect the global physiology of the *nqr nhaA* suppressors,
343 we performed comparative proteome analyses. For this purpose, we cultivated the parental
344 strain and the suppressors S3 (P_{pepA}), S5 (*pepA*) and S7 (P_{nhaB}) in LB medium under non-
345 selective conditions. As a control, we also compared the proteomes of an *E. coli* strain and its
346 isogenic *pepA* mutant. It is known that PepA represses the *carAB* operon that encodes the
347 CarAB carbamoylphosphate synthetase complex, which is involved in pyrimidine biosynthesis
348 [47,49-51]. Therefore, we expected that there would be less of CarA and CarB in *E. coli* and
349 possibly also in the *V. cholerae* suppressors S3 and S5. Indeed, both proteins were much less
350 abundant in the *E. coli pepA* mutant and in the two *nqr nhaA* suppressors (**Figure 5A**).
351 Interestingly, in the *E. coli pepA* mutant, the PyrIB enzyme complex was less abundant as
352 compared to the parental strain. PyrIB is also involved in pyrimidine biosynthesis and catalyzes
353 the reaction that follows CarAB. In the *V. cholerae* mutants S3 (P_{pepA} (-162ΔT)) and S4 (*pepA*
354 (G676T)), as expected, PepA abundance was strongly reduced. In contrast, suppressor S7
355 (P_{nhaB} (G-189A); **Figure 5B**) showed no changes in PepA abundance. Furthermore, the
356 comparative proteome analyses suggest different metabolic strategies of the suppressor
357 mutants to counteract Na^+ stress (**Figure 5B**, supplemental material Table S1). For example,
358 in suppressor S7 carrying a mutation in the *nhaB* promotor, which results in increased *nhaB*
359 expression (**Figure 3B**), there is a more than two-fold increase in levels of citrate lyase
360 subunits CitF and CitC and oxaloacetate decarboxylase subunits OadA-2 and OadG, which
361 are part of the *cit* operon allowing citrate fermentation [52]. Moreover, the malate synthase
362 AceB is highly overexpressed, likely further facilitating oxaloacetate biosynthesis from
363 isocitrate via the glyoxylate cycle. This will increase overall Na^+ export capacity with help of
364 the OadA-2 sodium pump [20] and might decrease carbon flux into the TCA cycle. In contrast,
365 in suppressors S3 (P_{pepA} (-162ΔT)) and S4 (*pepA* (G676T)), in which either expression of the
366 *pepA* promoter is impaired (**Figure 4C**) or truncated PepA is expressed, carbon flux through
367 the TCA cycle might be increased. Both the citrate lyase subunits (CitF in S3 and S4 and in

368 S4 also CitD) and OadA-2 (S3 and S4) are less abundant in these mutants, while at the same
369 time there is a moderate increase in citrate synthase subunit GltA in S4. Furthermore, in S4
370 the fumarase FumC is moderately less abundant, while the succinate-ubiquinone
371 oxidoreductase complex SdhAB is moderately more abundant. Interestingly, in line with
372 increased abundance of TCA cycle enzymes, enzymes involved in amino acid biosynthetic
373 pathways, especially for glutamate, tryptophan, glutamine, histidine and others are also more
374 abundant. Moreover, moderately increased levels of the ATP synthase are observed. This
375 suggests that an increase in membrane potential due to respiratory activity in suppressor S3
376 and especially S4 facilitates Na^+ export by the remaining Na^+/H^+ antiporters. This is probably
377 accompanied by changes in the membrane structure in suppressor S4, as indicated by
378 alterations in the protein levels of cell-envelope related proteins such as NlpC, CpxP, MinCD
379 (Supplemental material Table S1). However, the shapes of the *V cholerae* reference strain,
380 and of *V. cholerae nqr nhaA* and its suppressor strains, did not differ significantly
381 (Supplemental material **Figure 1**). Changes in abundance of the Na^+/H^+ antiporter NhaB itself
382 could not be identified. This is not surprising because NhaB is an integral membrane protein
383 with low recovery. To conclude, the proteome analyses revealed that the mutation in the P_{pepA}
384 promoter (S3) and in *pepA* (S4), reduce the cellular amount of PepA. Moreover, PepA also
385 regulates *carAB* expression in *V. cholerae* and changes in the proteomes indicated different
386 adaptation strategies of the *pepA* and *nhaB* suppressor mutants.
387
388
389
390
391
392
393
394
395
396

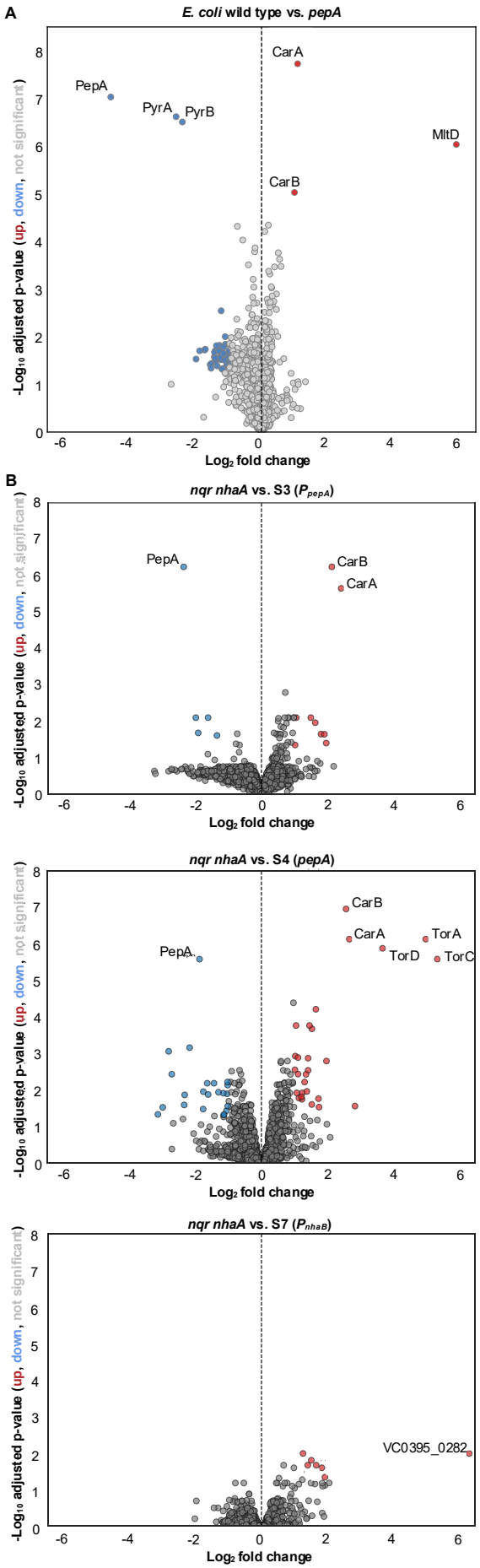

Figure 5. Comparative proteome profiling and chromosomal PepA binding sites. Proteome comparisons of the *E. coli* wild type (DS941) and *pepA* mutant (SDC1) strains (**A**) and of the *V. cholerae nqr nhaA* mutant and suppressors S3, S4 and S7 (**B**).

428 **Discussion**

429 In the present study, we found that the *V. cholerae nqr nhaA* mutant with impaired Na^+/H^+
430 homeostasis is genomically unstable during growth in the presence of elevated Na^+
431 concentrations at alkaline pH. Similarly, like the *V. cholerae nqr nhaA* mutant, an *E. coli nhaA*
432 *nhaB* mutant lacking the two specific Na^+/H^+ antiporters rapidly forms suppressor mutants at
433 high salinity [53]. The characterization of one of these suppressor mutants revealed that the
434 Na^+ export capacity was partially restored and the growth rate was like that of the wild type.
435 Although the genomic alteration allowing the growth of this mutant at elevated Na^+
436 concentrations was not identified, it was suggested that under some conditions *E. coli* can
437 synthesize a primary Na^+ pump when the Na^+/H^+ antiporters NhaA and NhaB are not present
438 [53]. It is tempting to speculate that the *E. coli nhaA nhaB* mutant was relieved by a mutation
439 that would affect the synthesis of the other known Na^+/H^+ antiporters like ChaA, MdfA and
440 MdtM [54-56]. However, in contrast to the Na^+-sensitive *E. coli nhaA nhaB* mutant, in
441 *V. cholerae*, the overproduction of the Na^+/H^+ antiporter NhaB can be achieved either by
442 overexpression of the *nhaB* gene or by mutations that affect the synthesis of PepA, a
443 multifunctional protein that has been extensively studied in *E. coli*. PepA was first identified as
444 an aminopeptidase that allows *E. coli* to utilize peptides as nutrient sources [57]. Interestingly,
445 PepA is also a component of a plasmid dimer resolution system that contributes to the
446 segregational and inheritable stability of natural plasmids like ColE1 [58]. PepA, together with
447 the DNA-binding regulator or arginine biosynthesis ArgR, serve as accessory proteins,
448 ensuring that the XerCD recombinase-dependent plasmid dimer to monomer conversion
449 occurs exclusively unidirectional [50,59-66]. Recently, it has been observed that PepA might
450 even serve as an RNA-binding chaperone in *E. coli* [67]. Moreover, PepA and ArgR are
451 required for stable maintenance of the P1 prophage and the repression of the *carAB* operon
452 in *E. coli* [47,49-51,68]. Thus, PepA can be assigned to the class of trigger enzymes, a group
453 of moonlighting proteins that are active in metabolism and in controlling gene expression
454 [69,70]. The regulation of gene expression by trigger enzymes can be achieved by direct
455 binding to DNA or RNA, by modulating the activity of a DNA-binding transcription factor or by

456 covalent modification of a transcription factor [69,70]. In many cases, the regulatory activity of
457 a trigger enzymes is controlled by the presence or absence of a substrate or cofactor. For
458 instance, the aconitase catalyses the reversible conversion of citrate to isocitrate in the
459 tricarboxylic acid cycle and requires an iron-sulphur cluster for activity [71]. Under conditions
460 of iron limitation, the aconitase binds to iron-responsive elements in the mRNAs of genes
461 involved in iron homeostasis [72]. However, in contrast to the aconitase, PepA does not require
462 any pyrimidine cofactor to bind to DNA *in vitro* [49]. Moreover, the structural characterisation
463 and the identification of PepA variants with single and multiple amino acid exchanges revealed
464 that the peptidase activity of the protein is not required for its DNA-binding and XerCD site-
465 specific recombination activity [47-49,73-76].

466 Recently, in *E. coli* and *V. cholerae* it has been shown that the available carbon source
467 affects the cellular localization of PepA and its DNA-binding activity [38]. In the presence of
468 glucose, a carbon source that allows rapid growth, PepA is sequestered to the membrane by
469 a direct interaction with the global transcription regulator CAP [38]. During nutrient-limited
470 growth (e.g., growth with acetate as the carbon source), PepA is released from the membrane
471 and becomes active as a DNA-binding transcription factor. It has been hypothesized that the
472 release of PepA from the membrane tailors a stress response to a nutrient-limited environment
473 [38]. ChIP-seq analyses identified 293 binding sites for PepA on the two chromosomes of *V.*
474 *cholerae* O1 biovar El Tor str. N16961, among them the P_{nhaB} and P_{pepA} promoter regions
475 (**Figure 3A, 4A** and supplemental material **Figure 2**) [Gibson et al., 2022]. Our suppressor
476 analysis supports the finding that PepA is a regulator of gene expression and Na^+/H^+
477 homeostasis in *V. cholerae* (**Figure 6**). The results of our comparative proteome study
478 obtained with derivatives of *V. cholerae* O395 compare favorably with the findings of Gibson
479 *et al*. 2022 [38], who identified PepA DNA binding sites in *V. cholerae* N16961. In many cases,
480 PepA binding revealed by ChIP-seq occurred upstream of genes, which are also affected in
481 our suppressor strains, as identified by proteomics (Table S1). In other cases, changes in
482 protein abundance are likely needed to redirect the flux of metabolites, e.g. towards the
483 nitrogen metabolism to prevent bottlenecks or imbalances due to high expression of e.g.

484 CarAB. Some proteins with higher abundance that may directly regulated by PepA are, for
485 example, the glutamate synthase GltB and PurDH enzyme complex (moderately increased)
486 that are involved in purine biosynthesis. Their expression likely needs to be coordinated with
487 CarAB to prevent metabolic imbalances. PepA also appears to be involved in the control of
488 toxin gene expression in *V. cholerae* O395 [77]. Thus, PepA links carbon source availability to
489 virulence in *V. cholerae*, a phenomenon that has been observed in many other pathogenic
490 bacteria [78].

491 As for *V. cholerae,* the PepA binding landscape in *E. coli* was globally mapped by ChIP-
492 seq [38,79]. In contrast to *V. cholerae*, *E. coli* PepA belongs to the group of transcription factors
493 and only binds to two promotors, thereby controlling its own synthesis and the expression of
494 the *carAB* operon [49,80]. The influence of PepA on the cellular concentrations of the PyrIB
495 complex and the membrane-bound lytic murein transglycosylase D (MtlD) is novel and
496 deserves further investigation (**Figure 5A**). In *Vibrio anguillarum*, MtlD has been associate with
497 virulence of the fish pathogen [81]. To conclude, PepA is a fascinating protein, and further
498 investigations will be necessary to decipher the significance of this multitasking protein for the
499 global bacterial physiology.

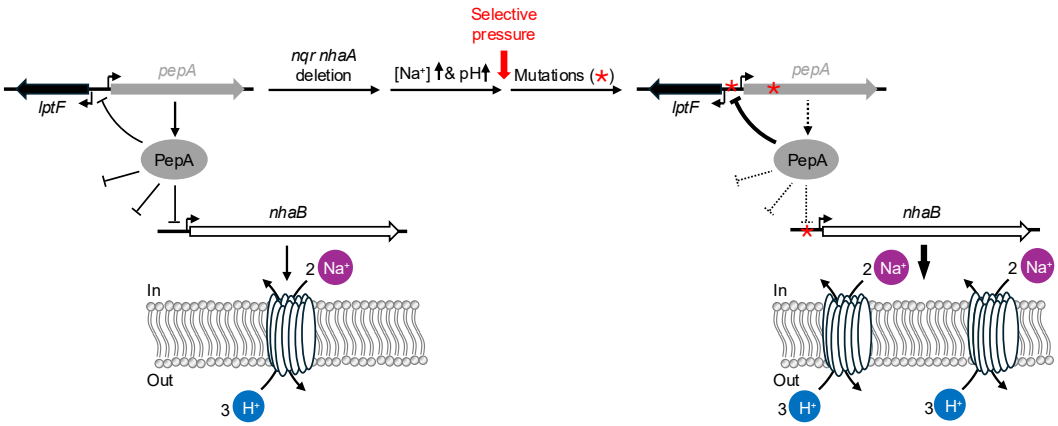

500
501 **Figure 6 Model for the regulation of the P_{nhaB} promoter by PepA.**
502 The cultivation of the *nhaA nqr* mutant under selection (high salinity and alkaline pH) causes
503 the accumulation of mutations that affect *pepA* expression, the cellular amount of PepA, and
504 *nhaB* expression.
505

506

507

508 **MATERIALS AND METHODS**

509 **Bacterial strains and chemicals**

510 Bacteria and oligonucleotides (purchased from Sigma-Aldrich, Munich, Germany) used in this
511 study are listed in Table 2. Chemicals and media were purchased from Sigma-Aldrich (Munich,
512 Germany), Carl Roth (Karlsruhe, Germany) and Becton Dickinson (Heidelberg, Germany).
513 Bacterial chromosomal DNA was isolated using the peqGOLD bacterial DNA kit (Peqlab,
514 Erlangen, Germany). PCR products were purified using the PCR purification kit (Qiagen,
515 Germany; New England Biolabs). Phusion DNA polymerase was purchased from Thermo
516 Scientific (Germany) and used according to the manufacturer's instructions.

517 **Cultivation of *E. coli* and *V. cholerae***

518 *E. coli* was grown in lysogeny broth (LB) at 37°C [82,83]. Agar plates were prepared with 15 g
519 agar/l (Roth, Germany). *E. coli* cells that were transformed with the plasmid pAC7 and its
520 derivatives were selected and LB plates supplemented with 100 µg/ml ampicillin and 80 µg/ml
521 X-Gal. *V. cholerae* was grown in LB, $LB_{sucrose}$, LB_{Tris}, and LB_{Tris}-NaCl medium. LB medium
522 contains 1 % tryptone (w/v), 0.5 % yeast extract (w/v), 171 mM NaCl and has a pH of 6.2.
523 $LB_{sucrose}$ contains 1 % tryptone (w/v), 0.5 % yeast extract (w/v) and 10 % sucrose (w/v)]. LB_{Tris}
524 medium was used to monitor the effect of Na^+ on the growth and contains 100 mM Tris. The
525 pH was adjusted to 7.6 with HCl at room temperature, which corresponds to pH 7.8 at 30 °C.
526 The Na^+ concentration of this medium was determined to be 13 mM using atomic absorption
527 spectroscopy. LB_{Tris}-NaCl medium was supplemented with 150 mM NaCl. *V. cholerae* strains
528 were grown at 30°C and selected with 50 µg/ml streptomycin. Growth of *V. cholerae* strains in
529 liquid medium at 30°C was monitored in 24-well plates (Thermo Scientific, USA) in an Infinite
530 F200 Pro plate reader (Tecan, Switzerland), and the OD_{595} was measured in 10 min intervals
531 for 24 h. For this purpose, the *V. cholerae* strains were cultivated overnight in LB_{Tris} medium at
532 180 rpm and 30°C. The cultures were normalized to an OD_{600} of 0.8. Next, a 24-well-plate was
533 prepared with 1 ml of growth medium in triplicates. After inoculation with 10 µl (1 %) of the
534 normalized overnight culture, growth was monitored with the plate reader.

535

536 **Plasmid construction**

537 Plasmids used and constructed in this study are listed in Table 2. Translational promoter-*lacZ*
538 fusions for determining the activities of the P_{nhaB}, P_{pepA} and P_{pepA} wild type and mutated
539 promoters were constructed as follows. The P_{nhaB}, P_{pepA} and P_{lptF} promoters were amplified by
540 PCR using the oligonucleotide pairs FMC15/FMC16, FMC23/FMC24 and FMC25/FMC26,
541 respectively. The primer pair FMC15/FMC49 was used to amplify the P_{nhaB} promoter variant
542 from suppressor S18. The P_{nhaB} promoter fragments (615 bp) were digested with *Eco*RI and
543 *Bam*HI and ligated with pAC7 [84] that was cut with the same enzymes. P_{pepA} and P_{lptF} (193
544 bp) promoter fragments were digested with *Eco*RI and *Bgl*II and ligated to the *Eco*RI/*Bam*HI-
545 linearized pAC7 plasmid. All generated plasmids were verified by Sanger sequencing
546 (Microsynth-SeqLab Sequence Laboratories, Göttingen, Germany).

547 **Construction of *V. cholerae nhaA* and *nqr nhaA* mutants**

548 The nontoxic variant of the *V. cholerae* Ogawa 395 strain (O395-N1) denoted "wild type"
549 [85,86] and the *nqr* mutant, a derivative of the strain O395-N1, lacking the *ABCDEF* operon
550 [87] were used as parental strains (Table 2). The plasmid pWM91 *nhaA* was isolated from the
551 *E. coli* strain SM10λ*pir* and used for transformation of the *E. coli* strain MFD*pir*. To obtain a
552 chromosomal deletion of the *nhaA* gene in *V. cholerae*, plasmid pWM91 *nhaA* was transferred
553 to the *V. cholerae* wild type and *nqr* mutant by conjugation using the *E. coli* donor strain
554 MFD*pir*-pWM91 *nhaA*. The *V. cholerae nhaA* and *V. cholerae nqr nhaA* mutants were selected
555 on $LB_{sucrose}$ medium and deletion of the *nhaA* gene was confirmed by colony PCR with the
556 oligonucleotide pair nhaA fwd/nhaA rev.

557 **Membrane potential measurements**

558 Membrane potential of *V. cholerae* cells was measured using the BacLight bacterial membrane
559 potential kit (Invitrogen) as described before [88]. Briefly, bacteria were grown in LB_{Tris}-NaCl
560 (30 °C, 180 rpm shaking) for 4 h, harvested (20 000 x g, 5 min, room temperature), washed in
561 PBS (137 mM NaCl, 2.7 mM KCl, 10 mM Na_2HPO_4, 1.8 mM K_2HPO_4, pH 7.4) and adjusted to
562 an OD_{600} of 0.25. Depolarisation control was achieved by addition of 5 µM CCCP (carbonyl
563 cyanide 3-chlorophenylhydrazone) and incubation for 15 min in the dark at 22 °C. Cell

564 suspensions without $DiOC_2$ (3,3′-diethyloxa-carbocyanine iodide) and with DMSO served as
565 controls. Staining was performed with 30 µM of $DiOC_2$. Samples (200 µL) from three different
566 cultures per strain were measured in black-bottomed 96-well plates (polystyrene, 4titude) in a
567 Tecan infinite F200 Pro plate reader (excitation: 485 nm / 20 nm: emission: 535 nm / 25 nm,
568 635 nm / 35 nm). Background fluorescence of cell suspension without $DiOC_2$ was subtracted.
569 Fluorescence intensities were normalised to that obtained with the wild type strain.

570 **Genome sequencing and plotting of PepA binding sites.**

571 Genomic DNA was prepared from 2 ml overnight cultures (LB_{Tris}-NaCl) using the peqGOLD
572 Bacterial DNA Kit (VWR, USA) following the instruction manual. Purified genomic DNA was
573 paired end sequenced (2 x 150 bp) (Azenta, Leipzig, Germany). Sequencing reads were
574 mapped to the *V. cholerae* genome (chromosome 1, CP000626.1; chromosome 2,
575 CP000627.1) using the Geneious (v. 2025.2.2, Docmatics) software package [89]. Genomic
576 regions of PepA binding sites (chromatin immune precipitation (ChIP) experiments published
577 by [38], Table S2) of *V. cholerae* O1 biovar El Tor str. N16961 (NC_002505.1 for chromosome
578 1 and NC_002506.1 for chromosome 2) were extracted and mapped to the genome of *V.*
579 *cholerae* O395-N1 (CP000627 for chromosome 1 and CP000626 for chromosome 2) using
580 the Geneious (v. 2025.2.2, Docmatics) software package (89 % similarity (cost matrix 93 %
581 similarity (5.0/-9.026168) and „only transfer best match“ settings) [89].

582 **β-Galactosidase assay**

583 Quantitative studies of *lacZ* expression in *E. coli* were performed as follows: cells were grown
584 at 37 °C in LB Medium. Cells were harvested at an optical density OD_{600} of 0.6 to 0.8. Specific
585 β-galactosidase activities were determined with cell extracts obtained by lysozyme treatment
586 as described previously [90]. One unit of β-galactosidase is defined as the amount of enzyme
587 which produces 1 nmol of *o*-nitrophenol per min at 28 °C. The BioRad dye-binding assay was
588 used to determine the protein concentrations.

589 **Electron microscopy**

590 Bacterial cultures were grown at 30 °C in LB medium for 4 h. Cells were harvested (13 000 x
591 g, 5 min, 4 °C) and resuspended in PBS. Samples were adjusted to an OD_{600} of 0.1 and

592 washed twice in PBS. Cells were fixed in fixative solution (50 mM HEPES pH 7.2, 1 % p-
593 formaldehyde, 2.5 % glutaraldehyde) for at least 2 h. After fixation, samples were gently
594 washed three times in PBS (13 000 x g, 5 min, 4 °C) and applied on poly-L-lysine coated glass-
595 slides. After stepwise dehydration in an ethanol series (5 min in each 30 %, 50 %, 70 %, 80 %,
596 90 %, 96 % EtOH), samples were critical point dried in CO_2 (K850 Critical Point Dryer, Quorum,
597 United Kingdom) coated with 8 nm carbon (Q 150 T ES plus, Quorum, United Kingdom) and
598 examined with a scanning electron microscope (EVO 15, Everhart-Thormley-Detector, Zeiss,
599 Oberkochen, Germany) at 8 kV and a sample current of 150 pA.

600 **Proteome analyses**

601 Bacterial cultures were grown at 30 °C in LB medium for 4 h. Cells were harvested (13 000 x
602 g, 5 min, 4 °C) and resuspended in PBS. Cell pellets were lysed in 60 µl trifluoroacetic acid at
603 70 °C for 3 minutes, before 600 µl of 2 M Tris Base was added. The cell lysates were cleared
604 by centrifugation for 5 minutes 16 000 x g at 4 °C. Protein concentrations of the cleared lysates
605 were determined by NanoDrop, and 10 µg of the proteins was subjected to tryptic digestion
606 (1:100 for 18 h at 37 °C). The peptides were desalted on Evotip™ using the standard producer
607 protocol and washed twice with 100 µl solvent A (0.1 % TFA (v/v) in water). Peptides were
608 eluted twice in solvent B (80 % ACN, 0.1 % TFA (v/v) in water) and vacuum dried. The samples
609 were resuspended in 20 µL 0.1 % (v/v) formic acid, 1.6 % (v/v) acetonitrile. For each
610 sample 0.4 µL injections were performed. The peptides were separated on a 50 cm µPAC Neo
611 HPLC Column (Thermo Scientific) operating at 50 °C column temperature. Mobile phase A
612 consisted of 0.1 % (v/v) formic acid and mobile phase B of 80 % v/v acetonitrile with 0.1% v/v
613 formic acid. After loading on the column peptides were separated first at a flow rate of 750 nL
614 min^{-1} for 4.95 minutes then 500 nL min^{-1} for 3.15 minutes. Separation was achieved using a
615 linear gradient from 4 % to 8 % mobile phase B over 0.25 minutes, then to 20% over 4.7
616 minutes, and subsequently to 35 % over 2.25 minutes. The gradient was followed by a rapid
617 increase to 99 % mobile phase B within 0.9 minutes. Eluted peptides were ionized by an
618 EASY-Spray source (Thermo Scientific) and introduced directly into the mass spectrometer.
619 The MS data were acquired in the data-independent (DIA) mode. For precursors with m/z

range of 380-980, isolated with 3 m/z isolation windows (0 overlap), resulting in 200 scan events per acquisition cycle. Isolated precursor ions were fragmented using higher-energy collisional dissociation (HCD) with a normalized collision energy of 25 %.MS2 spectra were recorded in the Astral mass analyzer over an m/z range of 150–2000. In parallel, one MS1 spectrum was acquired every 0.6 minutes in the Orbitrap at a resolution of 240 000 (at m/z 200) over an m/z range of 380–980.

Processing of mass spectrometry data

Raw files obtained from DIA runs were processed using DIA-NN 2.2.0. A FASTA file (UniProt *V. cholerae* serotype O1 reference proteome (Taxon ID: 243277) or *E. coli* (strain K12) reference proteome (Taxon ID: 83333)) was provided. A library-free search was enabled with Trypsin/P protease, 2 missed cleavages, peptide length range 7–30, precursor charge range 1–4, precursor m/z range 300–1800, fragment ion m/z range 200–1800. Cysteine carbamidomethylation was set as a fixed modification. Precursor FDR was set to 1 %, and MBR was activated. All other settings were left as default. Using the resulting “report.tsv” file as input, the data were uploaded to DIA Analyst v0.10.4 (https://analyst-suites.org/apps/dia-analyst/) with 0.05 as an adjusted *p*-value cutoff and 1 as log2 fold change cutoff. Imputation type was set to Perseus type with no normalization. Type of FDR correction was set to Benjamini–Hochberg. The resulting $\log_2$ fold changes and adjusted p-values were visualized in volcano-style scatter plots generated in Python (pandas, NumPy, matplotlib, seaborn). For each comparison, the $\log_2$ fold change (sign inverted for plotting) was plotted against the $-\log_{10}$-adjusted p-value. Proteins exceeding the fold-change and significance thresholds were highlighted by color. Features with $-\log_{10}$-adjusted *p*-values > 4, or alternatively the five most significant hits per regulation direction, were annotated using gene names with collision-avoiding label placement.

ACKNOWLEDGEMENTS

This work was supported by the University of Hohenheim. We are grateful to the members of the Commichau, Gibhardt and Steuber laboratories for helpful discussions. We thank Luise Weber for the help with some experiments. Support by grants 311211092 (to J.S. and G.F.) and 548311592 (to F.M.C.) from the Deutsche Forschungsgemeinschaft is gratefully acknowledged. S.H. thanks the Landesgraduiertenförderung Baden-Württemberg for financial support. Research reported in this publication was supported by National Institute of Allergy and Infectious Diseases of the National Institutes of Health under award number R03AI180583 (to C.C.H.). We are grateful to Sean Colloms, Daniel Charlier and Tadeusz Kaczorowski for providing plasmids, bacterial strains and helpful advice. We acknowledge the support provided by Susanne Reiße from the Imaging Module of the Core Facility Hohenheim (University of Hohenheim, Stuttgart, Germany) in electron microscopy analysis. Parts of the equipment used was supported by the EFRE EU fund (grant no. 2172959).

SUPPLEMENTAL MATERIAL

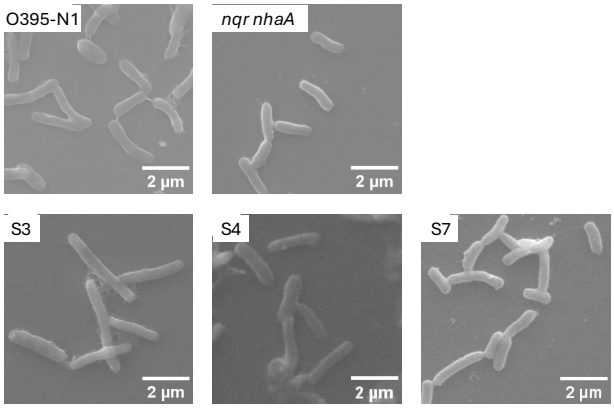

Supplemental Figure 1. Morphological characterization of *V. cholerae* strains. The strains were grown on LB (pH 6.2, 171 mM NaCl) to exponential phase, harvested and prepared for scanning electron microscopy. **Top panels:** *V. cholerae* O395-N1 (reference strain) and its variant *V. cholerae nqr nhaA* lacking the Na^+-NQR and the antiporter NhaA. **Bottom panels:** Suppressor mutants S3, S4 and S7 obtained after prolonged cultivation of *V. cholerae nqr nhaA* on LB_{Tris}-NaCl (pH 7.8, 150 mM NaCl). All strains were rod shaped and of similar size.

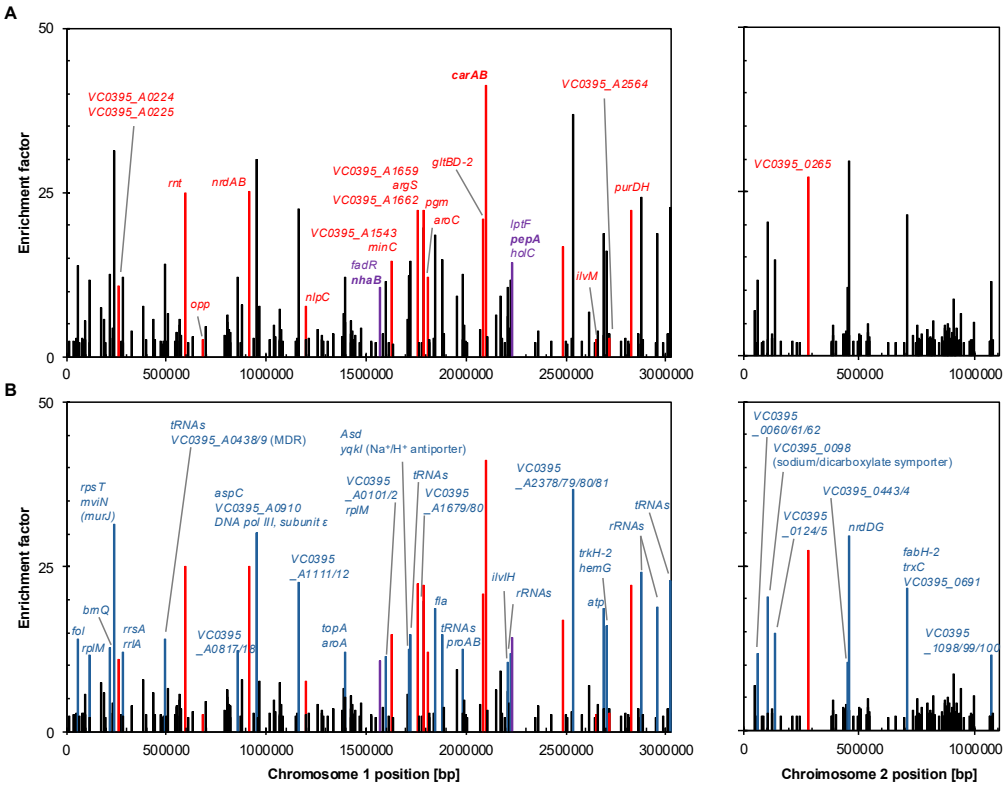

Supplemental Figure 2. Overlap between PepA binding sites and changes in protein abundance. (**A**) The PepA binding sites in *V. cholerae* O1 biovar El Tor str. N16961 were previously identified by chromatin immunoprecipitation sequencing (ChIP-Seq) [38]. To visualize their distribution across the chromosomes, the PepA binding sites were extracted and mapped onto the the genome of *V. cholerae* O395-N1. The enrichment factors of the binding sites obtained by ChIP-Seq are shown as bars. Red labelled bars indicate PepA binding sites of genes encoding proteins whose abundance was changed only in S3 or S4, or in both suppressors (fold change > 1 or < -1) ($p < 0.05$). Purple labelled bars indicate PepA binding sites in *fadR-nhaB* and *lptF-pepA* intergenic regions, and in the *holC* gene that is located downstream of *pepA*. (**B**) Blue bars indicate PepA binding sites of genes encoding proteins whose abundance remained unchanged.

711 **REFERENCES**

712

713 1. **Imae Y, Atsumi T** (1989) Na^+-driven bacterial flagellar motors. J Bioenerg
714 Biomembr 21: 705-716.
715 2. **Padan E, Schuldiner S** (1994) Molecular physiology of Na^+/H^+ antiporters, key
716 transporters in circulation of $Na^+$and H^+ in cells. Biochim Biophys Acta 1185:
717 129-151.
718 3. **Nakamura T, Komano Y, Itaya E, Tsukamoto K, Tsuchiya T, Unemoto T**
719 (1994) Cloning and sequencing of an Na^+/H^+ antiporter gene from the marine
720 bacterium *Vibrio alginolyticus*. Biochim Biophys Acta 1190: 465-468.
721 4. **Nakamura T, Enomoto H, Unemoto T** (1996) Cloning and sequencing of the
722 *nhaB* gene encoding an Na^+/H^+ antiporter from *Vibrio alginolyticus*. Biochim
723 Biophys Acta 1275: 157-160.
724 5. **Nozaki K, Inaba K, Kuroda T, Tsuda M, Tsuchiya T** (1996) Cloning and
725 sequencing of the gene for Na^+/H^+ antiporter of *Vibrio parahaemolyticus*.
726 Biochem Biophys Res Commun 222: 774-779.
727 6. **Herz K, Vimont S, Padan E, Berche P** (2003) Roles of NhaA, NhaB Na^+/H^+
728 antiporters in survival of *Vibrio cholerae* in saline environment. *J Bacteriol* 185:
729 1236-1244.
730 7. **Masrati G, Dwivedi M, Rimon A, Gluck-Margolin Y, Kessel A, Ashkenazy**
731 **H, Mayrose I, Padan E, Ben-Tal N** (2018) Broad phylogenetic analysis of
732 cation/proton antiporters reveals transport determinants. Nat Commun 9: 4205.
733 8. **Patino-Ruiz M, Fendler K, Calinescu O** (2019) Mutation of two key aspartate
734 residues alters stoichiometry of the NhaB Na^+/H^+ exchanger from *Klebsiella*
735 *pneumoniae.* Sci Rep 9: 15390.
736 9. **Padan E, Maisler N, Taglicht D, Karpel R, Schuldiner S** (1989) Deletion of
737 *ant* in *Escherichia coli* reveals its function in adaptation to high salinity and an
738 alternative Na^+/H^+ antiporter system(s). *J Biol Chem* 264: 20297-20302.
739 10. **Pinner E, Padan E, Schuldiner S** (1992) Cloning, sequencing, and expression
740 of the *nhaB* gene, encoding a Na^+/H^+ antiporter in *Escherichia coli*. J Biol Chem
741 267: 11064-11068.
742 11. **Pinner E, Kotler Y, Padan E, Schuldiner S** (1993) Physiological role of NhaB,
743 a specific Na^+/H^+ antiporter in *Escherichia coli*. J Biol Chem 268: 1729-1734.
744 12. **Pinner E, Padan E, Schuldiner S** (1994) Kinetic properties of NhaB, a Na^+/H^+
745 antiporter from *Escherichia coli*. J Biol Chem 269: 26274-26279.
746 13. **Krulwich TA, Sachs G, Padan E** (2011) Molecular aspects of bacterial pH
747 sensing and homeostasis. Nat Rev Microbiol 9: 330-343.
748 14. **Karpel R, Alon T, Glaser G, Schuldiner S, Padan E** (1991) Expression of a
749 sodium proton antiporter (NhaA) in *Escherichia coli* is induced by Na^+ and Li^+
750 ions. J Biol Chem 266: 21753-21759.
751 15. **Rahav-Manor O, Carmel O, Karpel R, Taglicht D, Glaser G, Schuldiner S,**
752 **Padan E** (1992) NhaR, a protein homologous to a family of bacterial regulatory
753 proteins (LysR), regulates *nhaA*, the sodium proton antiporter gene in
754 *Escherichia coli*. J Biol Chem 267: 10433-10438.
755 16. **Dover N, Padan E** (2001) Transcription of *nhaA*, the main Na^+/H^+ antiporter of
756 *Escherichia coli*, is regulated by $Na^+$and growth phase. J Bacteriol 183: 644-
757 653.
758 17. **Demeester W, De Paepe B, De Mey M** (2024) Fundamentals and exceptions
759 of the LysR-type transcriptional regulators. ACS Synth Biol 13: 3069-3092.
760 18. **Dwivedi M, Sukenik S, Friedler A, Padan E** (2016) The Ec-NhaA antiporter
761 switches from antagonistic to synergistic antiport upon a single point mutation.

762 Sci Rep 6: 23339.
763 **19. Steuber J, Fritz G** (2024) The Na^+-translocating NADH:quinone
764 oxidoreductase (Na^+-NQR): Physiological role, structure and function of a
765 redox-driven, molecular machine. Biochim Biophys Acta Bioenerg 1865:
766 149485.
767 **20. Dahinden P, Pos KM, Dimroth P** (2005). Identification of a domain in the
768 alpha-subunit of the oxaloacetate decarboxylase Na^+ pump that accomplishes
769 complex formation with the gamma-subunit. FEBS J 272: 846–855.
770 **21. Hau JL, Kaltwasser S, Muras V, Casutt MS, Vohl G, Claußen B, Steffen W,**
771 **Leitner A, Bill E, Cutsail III GE, Vonck J, Steuber J, Fritz G** (2023)
772 Conformational coupling of redox-driven Na^+-translocation in *Vibrio cholerae*
773 NADH:quinone oxidoreductase. Nat Struct Mol Biol 30: 1686-1694.
774 **22. Mourin M, Schubiger CB, Resch CT, Häse CC, Dibrov P** (2017) Physiology
775 of the Vc-NhaP paralogous group of cation-proton antiporters in *Vibrio cholerae*.
776 Mol Cell Biochem 428: 87-99.
777 **23. Merrell DS, Hava DL, Camilli A** (2002) Identification of novel factors involved
778 in colonization and acid tolerance of *Vibrio cholerae*. Mol Microbiol 43: 1471-
779 1491.
780 **24. Walton MG, Cubillejo I, Nag D, Withey JH** (2023) Advances in cholera
781 research: from molecular biology to public health initiatives. Front Microbiol 14:
782 1178538.
783 **25. Häse CC, Mekalanos JJ** (1999) Effects of changes in membrane sodium flux
784 on virulence gene expression in *Vibrio cholerae*. Proc Natl Acad Sci USA 96:
785 3183-3187.
786 **26. Kaminski JW, Vera L, Stegmann DP, Vering J, Eris D, Smith KML, Huang**
787 **CY, Meier N, Steuber J, Wang M, Fritz G, Wojdyla JA, Sharpe ME** (2022)
788 Fast fragment- and compound-screening pipeline a the Swiss Light Source.
789 Acta Crystallogr D Struct Biol 78: 328-336.
790 **27. Lee BS, Singh S, Pethe K** (2023) Inhibiting respiration as a novel antibiotic
791 strategy. Curr Opin Microbiol 74: 102327.
792 **28. Vimont S, Berche P** (2000) NhaA, an Na^+/H^+ antiporter involved in
793 environmental survival in *Vibrio cholerae*. J Bacteriol 182: 2937-2944.
794 **29. Hunte C, Screpanti E, Venturi M, Rimon A, Padan E, Michel H** (2005)
795 Structure of a Na^+/H^+ antiporter and insights into mechanism of action and
796 regulation by pH. Nature 435: 1197-1202.
797 **30. Williams SG, Carmel-Harel O, Manning PA** (1998) A functional homolog of
798 *Escherichia coli* NhaR in *Vibrio cholerae*. J Bacteriol 180: 762-765.
799 **31. Dzioba J, Ostroumov E, Winogrodzki A, Dibrov P** (2002) Cloning, functional
800 expression in *Escherichia coli* and primary characterization of a new Na^+/H^+
801 antiporter, NhaD, of *Vibrio cholerae.* Mol Cell Biochem 229: 119-124.
802 **32. Quinn MJ, Resch CT, Sun J, Lind EJ, Dibrov P, Häse CC** (2012) NhaP1 is a
803 $K^+(Na^+)/H^+$ antiporter required for growth and internal pH homeostasis of *Vibrio*
804 *cholerae* at low extracellular pH. Microbiology (Reading). 158: 1094-1105.
805 **33. Dzioba-Winogrodzki J, Winogrodzki O, Krulwich TA, Boin MA, Häse CC,**
806 **Dibrov P** (2008) The *Vibrio cholerae* Mrp system: cation/proton antiport
807 properties and enhancement of bile salt resistance in a heterologous host. J Mol
808 Microbiol Biotechnol 16: 176-186.
809 **34. Minato Y, Fassio SR, Kirkwood JS, Halang P, Quinn MJ, Faulkner WJ,**
810 **Aagesen AM, Steuber J, Stevens JF, Häse CC** (2014) Roles of the sodium-
811 translocating NADH:quinone oxidoreductase (Na^+-NQR) on *Vibrio cholerae*
812 metabolism, motility and osmotic stress resistance. PLoS One 9: e97083.

35. **Schubiger CB, Häse CC** (2020) Growth assays of *Vibrio cholerae* membrane transporter mutants in different pH and cation conditions. J Mol Biol Biotechnol 5: 01.
36. **Sadovskaya NS, Laikov ON, Mironov AA, Gelfand MS** (2001) Study of regulation of long-chain fatty acid metabolism using computer analysis of complete bacterial genomes. Mol Biol 35: 1010-1014.
37. **Iram SH, Cronan JE** (2005) Unexpected functional diversity among FadR fatty acid transcriptional regulatory proteins. J Biol Chem 280: 32148-32156.
38. **Gibson JS, Gebhardt MJ, Santos RERS, Dove SL, Watnick PI** (2022) Sequestration of a dual DNA-binding protein by *Vibrio cholerae* CRP. Proc Natl Acad Sci USA 119: e2210115119.
39. **Okunishi I, Kawagishi I, Homma M** (1996) Cloning and characterization of *motY*, a gene coding for a component of the sodium-driven flagellar motor in *Vibrio alginolyticus*. J Bacteriol 178: 2409-2415.
40. **Brown II, Häse CC** (2001) Flagellum-independent surface migration of *Vibrio cholerae* and *Escherichia coli*. J Bacteriol 183: 3784-3790.
41. **Pal RR, Das B, Dasgupta S, Bhadra RK** (2011) Genetic components of stringent response in *Vibrio cholerae.* Indian J Med Res 133: 212-217.
42. **Potts AH, Vakulskas CA, Pannuri A, Yakhnin H, Babitzke P, Romeo T** (2017) Global role of the bacterial post-transcriptional regulator CsrA revealed by integrated transcriptomics. Nat Commun 8: 1596.
43. **Dormeyer M, Lübke AL, Müller P, Lentes S, Reuß DR, Thürmer A, Stülke J, Daniel R, Brantl S, Commichau FM** (2017) Hierarchical mutational events compensate for glutamate auxotrophy of a *Bacillus subtilis gltC* mutant. Environ Microbiol Rep. 9: 279-289.
44. **Gundlach J, Herzberg C, Hertel D, Thürmer A, Daniel R, Link H, Stülke J** (2017) Adaptation of *Bacillus subtilis* to life at extreme potassium limitation. mBio 8: e00861-17.
45. **Wicke D, Schulz LM, Lentes S, Scholz P, Poehlein A, Gibhardt J, Daniel R, Ischebeck T, Commichau FM** (2019) Identification of the first glyphosate transporter by genomic adaptation. Environ Microbiol 21: 1287-1305.
46. **Owens TW, Taylor RJ, Pahil KS, Bertani BR, Ruiz N, Kruse AC, Kahne D** (2019) Structural basis of unidirectional export of lipopolysaccharide to the cell surface. Nature 567: 550-553.
47. **Charlier D, Kholti A, Huysveld N, Gigot D, Maes D, Thia-Toong TL, Glansdorff N** (2000) Mutational analysis of *Escherichia coli* PepA, a multifunctional DNA-binding aminopeptidase. *J Mol Biol* 302: 411-426.
48. **Reijns M, Lu Y, Leach S, Colloms SD** (2005) Mutagenesis of PepA suggests a new model for the Xer/cer synaptic complex. Mol Microbiol 57: 927-941.
49. **Charlier D, Hassanzadeh G, Kholti A, Gigot D, Pierard A, Glansdorff N** (1995) *carP*, involved in pyrimidine regulation of the *Escherichia coli* carbamoylphosphate synthetase operon encodes a sequence-specific DNA-binding protein identical to XerB and PepA, also required for resolution of ColEI multimers. *J Mol Biol* 250: 392-406.
50. **Minh PN, Devroede N, Massant J, Maes D, Charlier D** (2009) Insights into the architecture and stoichiometry of *Escherichia coli* PepA*DNA complexes involved in transcriptional control and site-specific DNA recombination by atomic force microscopy. Nucleic Acids Res 37: 1463-1476.
51. **Nguyen Le Minh P, Nadal M, Charlier D** (2016) The trigger enzyme PepA (aminopeptidase A) of *Escherichia coli*, a transcriptional repressor that generates positive supercoiling. FEBS Lett 590: 1816-1825.

52. **Liu M, Hao G, Li Z, Zhou Y, Garcia-Sillas R, Li J, Wang H, Kan B, Zhu J.** (2019) CitAB two-component system-regulated citrate utilization contributes to *Vibrio cholerae* competitiveness with the gut microbiota. Infect Immun 87: e00746-18.
53. **Harel-Brinstein M, Dibrov P, Olami Y, Pinner E, Schuldiner S, Padan** E (1995) MH1, a second-site revertant of an *Escherichia coli* mutant lacking Na^+/H^+ antiporters (Δ*nhaA* Δ*nhaB*), regains Na^+/H^+ resistance and a capacity to excrete Na^+ in a $\Delta\tilde{\mu}_{H^+}$-independent fashion. *J Biol Chem* 270: 3816-3822.
54. **Ivey DM, Guffanti AA, Zemsky J, Pinner E, Karpel R, Padan E, Schuldiner S, Krulwich TA** (1993) Cloning and characterization of a putative Ca^{2+}/H^+ antiporter gene from *Escherichia coli* upon functional complementation of a Na^+/H^+ antiporter-deficient strains by the overextpressed gene. J Biol Chem 268: 11296-11303.
55. **Lewinson O, Padan E, Bibi E** (2004) Alkalitolerance: a biological function for a multidrug transporter in pH homeostasis. Proc Natl Acad Sci USA 101: 14073-14078.
56. **Holdsworth SR, Law CJ** (2013) Multidrug resistance protein MdtM adds to the repertoire of antiporters involved in alkaline pH homeostasis in *Escherichia coli*. BMC Microbiol 23: 113.
57. **Sussman AJ, Gilvarg C** (1970) Peptidases in *Escherichia coli* K-12 capable of cleaving lysine homopeptides. J Biol Chem 245: 6518-6524.
58. **Colloms SD** (2013) The topology of plasmid monomerizing Xer site-specific recombination. Biochem Soc Trans 41: 589-594.
59. **Stirling CJ, Colloms SD, Collins JF, Szatmari G, Sherratt DJ** (1989) *xerB*, an *Escherichia coli* gene required for plasmid ColE1 site-specific recombination, is identical to *pepA*, encoding aminopeptidase A, a protein which substantial similarity to bovine lens leucine aminopeptidase. EMBO J 8: 1623-1627.
60. **Flinn H, Burke M, Stirling CJ, Sherratt DJ** (1989) Use of gene replacement to construct *Escherichia coli* strains carrying mutations in two genes required for stability of multicopy plasmids. J Bacteriol 171: 2241-2243.
61. **Colloms SD, Sykora P, Szatmari G, Sherratt DJ** (1990) Recombination at ColE1 cer requires the *Escherichia coli xerC* gene product, a member of the lambda integrase family of site-specific recombination. J Bacteriol 172: 6973-6980.
62. **Colloms SD, McCulloch R, Grant K, Neilson L, Sherratt DJ** (1996) Xer-mediated site-specific recombination *in vitro*. EMBO J 15: 1172-1181.
63. **Guhathakurta A, Summers D** (1995) Involvement of ArgR and PepA in the pairing of ColE1 dimer resolution. Microbiology (Reading). 141: 1163-1171.
64. **Guhathakurta A, Viney I, Summers D** (1996) Accessory proteins impose site selectivity during ColE1 dimer resolution. Mol Microbiol 20: 613-620.
65. **Alén C, Sherratt DJ, Colloms SD** (1997) Direct interaction of aminopeptidase A with recombinant DNA in Xer site-specific recombination. EMBO J 16: 5188-5197.
66. **Charlier D, Bervoets I** (2019) Regulation of arginine biosynthesis, catabolism and transport in *Escherichia coli*. Amino Acids 51: 1103-1127.
67. **Rojano-Nisimura AM, Miller LG, Anantharaman A, Middleton AT Kibret E, Jung SH, Russel R, Contreras LM** (2024) A high-throughput search for intracellular factors that affect RNA folding identifies *E. coli* proteins PepA and YagL as RNA chaperones that promote RNA remodeling. RNA Biol 21: 13-30.
68. **Paul S, Summers D** (2004) ArgR and PepA accessory proteins for XerCD-mediated resolution of ColE1 dimers, are also required for stable maintenance

of the P1 prophage. Plasmid 52: 63-68.

69. **Commichau FM, Stülke J** (2008) Trigger enzymes: bifunctional proteins active in metabolism and in controlling gene expression. *Mol Microbiol* 67: 692-702.
70. **Commichau FM, Stülke J** (2015) Trigger enzymes: coordination of metabolism and virulence gene expression. Microbiol Spectr 3: doi: 10.1128/microbiolspec.MBP-0010-2014.
71. **Beinert BR, Kennedy MC, Stout CD** (1996) Aconitase as iron-sulfur protein, enzyme, and iron-regulatory protein. Chem Rev 96: 2335-2374.
72. **Kaptain S, Downey WE, Tang C, Philpott C, Haile D, Orloff DG, Harford JB, Rouault TA, Klausner RD** (1991) A regulated RNA binding protein also possesses aconitase activity. Proc Natl Acad Sci USA 88: 10109-10113.
73. **Summers DK, Sherratt DJ** (1988) Resolution of ColE1 dimers requires a DNA sequence implicated in the three-dimensional organization of the *cer* site. Embo J 7: 851-858.
74. **McCulloch R, Burke ME, Sherratt DJ** (1994) Peptidase activity of *Escherichia coli* aminopeptidase A is not required for its role in Xer site-specific recombination. Mol Microbiol 12: 241-251.
75. **Sträter N, Sherratt DJ, Colloms SD** (1999) X-ray structure of aminopeptidase A from *Escherichia coli* and a model for the nucleoprotein complex in Xer site-specific recombination. EMBO J 18: 4513-4522.
76. **Devroede N, Huysveld N, Charlier D** (2006) Mutational analysis of intervening sequences connecting the binding site for integration host factor, PepA, PurR, and RNA polymerase in the control region of the *Escherichia coli carAB* operon encoding carbamoylphosphate synthase. J Bacteriol 188: 3236-3245.
77. **Behari J, Stagon L, Calderwood SB** (2001) *pepA*, a gene mediating pH regulation of virulence genes in *Vibrio cholerae*. J Bacteriol 183: 178-188.
78. **Görke B, Stülke J** (2008) Carbon catabolite repression in bacteria: many ways to make the most out of nutrients. Nat Rev Microbiol 6: 613-624.
79. **Lally P, Gómez-Romero L, Tierrafría VH, Aquino P, Rioualen C, Zhang X, Kim S, Baniulyte G, Plitnick J, Smith C, Babu M, Collado-Vides J, Wade JT, Galagan JE** (2025) Predictive biophysical neural network modeling of a compendium of *in vivo* transcription factor DNA binding profiles for *Escherichia coli*. Nat Commun 16: 4255.
80. **Shimada T, Ogasawara H, Kobayashi I, Kobayashi N, Ishihama A** (2021) Single-target regulators constitute the minority group of transcription factors in *Escherichia coli* K-12. Front Microbiol 12: 697803.
81. **Xu Z, Wang Y, Han Y, Chen J, Zhang XH** (2011) Mutation of a novel virulence-related gene *mltD* in *Vibrio anguillarum enhances* lethality in zebra fish. Res. Microbiol. 162: 144-150.
82. **Miller JH** (1972) Experiments in molecular genetics. Cold Spring Harbour Laboratory, Cold Spring Harbour, NY. 466pp.
83. **Sezonov G, Joseleau-Petit D, D'Ari R** (2007) *Escherichia coli* physiology in Luria-Bertani broth. *J Bacteriol* 8746-8749.
84. **Weinrauch Y, Msadek T, Kunst F, Dubnau D** (1991) Sequence and properties of *comQ*, a new competence regulatory gene of *Bacillus subtilis*. *J Bacteriol* 173: 5685-5693.
85. **Mekalanos JJ, Schwartz DJ, Pearson GD, Harford N, Groye F, de Wilde M** (1983) Cholera toxin genes: nucleotide sequence, deletion analysis and vaccine development. Nature 306: 551-557.
86. **Häse CC, Mekalanos JJ** (1998) TcpP protein is a positive regulator of virulence gene expression in *Vibrio cholerae.* Proc Natl Acad Sci USA 95: 730-734.

87. **Barquera B, Hellwig P, Zhou W, Morgan JE, Häse CC, Gosink KK, Nilges M, Bruesehoff PJ, Roth A, Lancaster CRD, Gennis RB** (2002) Purification and characterization of the recombinant Na^+-translocating NADH:quinone oxidoreductase from *Vibrio cholerae.* Biochemistry 41: 3781-3789.
88. **Vorburger T, Nedielkov R, Brosig A, Bok E, Schunke E, Steffen W, Mayer S, Götz F, Möller HM, Steuber J** (2016) Role of the Na^+-translocating NADH:quinone oxidoreductase in voltage generation and Na^+ extrusion in *Vibrio cholerae*. Biochim Biophys Acta 1857: 473-482.
89. **Kearse M, Moah R, Wilson A, Stones-Havas S, Cheung M, Sturrock S, Buxton S, Cooper A, Markowitz S, Duran C, Thierer T, Ashton B, Meintjes P, Drummond A (**2012) Geneious Basic: An integrated and extendable desktop software platform for the organization and analysis of sequence data. Bioinformatics 28: 1647-1649.
90. **Kunst F, Rapoport G** (1995) Salt stress is an environmental signal affecting degradative enzyme synthesis in *Bacillus subtilis*. J Bacteriol, 177: 2403-2407.
91. **Schulz H, Hennecke H, Thöny-Maier L** (1998) Prototype of a heme chaperone essential for cytochrome c maturation. Sience 281: 1197-1200.
92. **Jackson SA, Fellows BJ, Fineran PC** (2020) Complete genome sequences of the *Escherichia coli* donor strains ST18 and MFD*pir*. Microbial Resour Announc 9: e01014-20.
93. **Miller VL, Mekalanos JJ** (1988) A novel suicide vector and its use in construction of insertion mutations: osmoregulation of outer membrane proteins and virulence determinants in *Vibrio cholerae* requires *toxR*. J Bacteriol 170: 2575-2583.

Supplemental material

Table S1. Results of proteome analyses.

997

Table 1. Isolated *V. cholerae nqr nhaA* suppressor mutants		
Suppressor	**Genotype[a]**	**Effect of the mutation(s)**
S1	*pepA* (G1303T) *rpoD* (C1268T) *dgt* (C686A)	PepA (D435Y) RpoD (A423V) Dgt (S229Y)
S2	P_{nhaB} (-361T^{Ins})	Altered *nhaB* expression
S3	P_{pepA} (-162ΔT)	Altered *pepA* expression
S4	*pepA* (G676T)	PepA (Δ226-503)
S5	*pepA* (G676T)	PepA (Δ226-503)
S6	*pepA* (G676T)	PepA (Δ226-503)
S7	P_{nhaB} (G-189A)	Altered *nhaB* expression
S8	*pepA* (T470A)	PepA (Δ157-503)
S9	P_{pepA} (-162ΔT)	Altered *pepA* expression
S10	P_{nhaB} (G-189A)	Altered *nhaB* expression
S11	*pepA* (G491T) *csrA* (A31C)	PepA (R164L) CsrA (T11P)
S12	*pepA* (G491T) *csrA* (A31C)	PepA (R164L) CsrA (T11P)
S13	*pepA* (G491T) *csrA* (A31C)	PepA (R164L) CsrA (T11P)
S14	*pepA* (C490A) P_{nhaB} (Δ-388 – -361 (ΔAATAAACTTACTCGAAAGAGGTATTTCT)) Δ71878-72267 (tRNA^{Arg} (VC0395_A0077) tRNA^{Ser} (VC0395_A0078) tRNA^{Arg} (VC0395_A0079))	PepA (R164S), increased expression of *nhaB*, [tRNA^{Arg} tRNA^{Ser}] decreased?
S15	*pepA* (T482A) VC0395_A2444 (134ΔA) *motY* (C604A)	PepA (V161E), VC0395_A2444 (V46C P47H Δ48-94), MotY (R202S)
S16	P_{nhaB} (A-345G) *pilA* (G221A)	Altered *nhaB* expression, PilA (G74D)
S17	P_{nhaB} (A-345G)	Altered *nhaB* expression
S18	P_{nhaB} (A-12G) *secA* (Δ2233 – 2262 (ΔGAGGTTTATAAAGCCAAAGAGCAAGCGGTT)) VC0395_0946 (1013_1014 ins ACCAGA)	Altered *nhaB* expression, SecA (ΔE741 – K750), VC0395_0946 (338_339 ins PE)
S19	P_{nhaB} (A-12G) *spoT* (C1176A)	Altered *nhaB* expression, SpoT (F392L)
S20	P_{nhaB} (A-12G) *rpoB* (C2623T) VC0395_0028 (C498T)	Altered *nhaB* expression, RpoB (R875C)

998 [a]The identified mutations are specified in relation to the start codon of the indicated genes.

Table 2. Oligonucleotides, plasmids and bacterial strains		
Oligonucleotide	**Sequence[a], 5' → 3'**	**Purpose**
IS95	CATCACAAACAGAATGATGTACCTG	Sequencing of pAC7 derivatives
IS96	GCAACTGTTGGGAAGGGCG	Sequencing of pAC7 derivatives
FMC15	AAAGAATTCGTCGAATGGCACTCATCATACCACTAGTTG	Amplification of the P_{nhaB} promoter
FMC16	TTTGGATCCATGATGATTACTCTTTAACTGTTGTTATAGATAGACTTTGTG	Amplification of the P_{nhaB} promoter
FMC23	AAAGAATTCCTAAAAACAGCACGAAGAAGATCGCAAACTGG	Amplification of the P_{pepA} promoter
FMC24	TTTAGATCTTCCATGCGTACTCCTACATCCTGAAGACAAATAG	Amplification of the P_{pepA} promoter
FMC25	AAAGAATTCGCGTATCCTCACTCCTGAAGACAAATAG	Amplification of the P_{lptF} promoter
FMC26	TTTAGATCTTCCTGGCTTTTTATTGTTTCTCGGATCAAATATCTAACAAATAATCAC	Amplification of the P_{lptF} promoter
FMC49	TTTGGATCCATGATGATTACTCCTTAACTGTTGTTATAGATAGACTTTGTG	Amplification of the P_{nhaB} promoter from *V. cholerae* S18
nhaA fwd	AAGCCTAGCTACACTCTGGAACA	Verification of the *nhaA* deletion
nhaA rev	CCGCGGTGGTTGACCCCATT	Verification of the *nhaA* deletion
Plasmids	**Purpose, insert**	**Reference**
pAC7	Empty plasmid, construction of translational *lacZ* fusions	[84]
pISC	Empty plasmid, expression of genes in *V. cholerae*	[21]
pNQR	Empty plasmid, expression of the *nqr* operon in *V. cholerae*	[91]
pBP570	P_{nhaB}-*lacZ*	This study
pBP571	P_{nhaB} (G-189A)-*lacZ*	This study
pBP575	P_{nhaB} (-361T^{ins})-*lacZ*	This study
pBP577	P_{pepA} (-162ΔT)-*lacZ*	This study
pBP578	P_{pepA}-*lacZ*	This study
pBP579	P_{lptF} (-26ΔA)-*lacZ*	This study
pBP580	P_{lptF}-*lacZ*	This study
pBP585	P_{nhaB} (A-345G)-*lacZ*	This study
pBP586	P_{nhaB} (A-12G)-*lacZ*	This study
pBP587	P_{nhaB} (Δ27)-*lacZ*	This study
Bacterial strains	**Purpose, genotype**	**Reference**
E. coli		
MFD*pir*	Host for pWM91 derivatives and conjugation	[92]
SM10λ*pir*	Host for pWM91 derivatives and conjugation	[93]
XL1-Blue	*recA1 endA1 gyrA96 thi-1 hsdR17 supE44 relA1 lac* [F´ *proAB lacI*^{q} *Z*Δ*M15* Tn*10*(*tet*^{R})]	Agilent

DS941	AB1157 *recF lacZ*Δ*M15*	[73]
SDC1	AB1157 *recF lacZ*Δ*M15 pepA::tet*^{R}	[73]
V. cholerae[b]		
O395-N1	Parental strain, *lacZ sm*^{R}	[85]
O395-N1 (TZ)	*lacZ sm*^{R} *toxT*::*lacZ*	[85]
nqr	*lacZ sm*^{R} *toxT*::*lacZ ctxA nqr*	[87]
nhaA	*lacZ sm*^{R} *toxT*::*lacZ ctxA nhaA*	[35]
nqr nhaA	*lacZ sm*^{R} *toxT*::*lacZ ctxA nqr nhaA*	[35]
S1	*lacZ sm*^{R} *toxT*::*lacZ ctxA nqr nhaA pepA* (G1303T) *rpoD* (C1268T) *dgt* (C686A)	This study
S2	*lacZ sm*^{R} *toxT*::*lacZ ctxA nqr nhaA* P_{nhaB} (-361T^{Ins})	This study
S3	*lacZ sm*^{R} *toxT*::*lacZ ctxA nqr nhaA* P_{pepA} (-162ΔT)	This study
S4	*lacZ sm*^{R} *toxT*::*lacZ ctxA nqr nhaA pepA* (G676T)	This study
S5	*lacZ sm*^{R} *toxT*::*lacZ ctxA nqr nhaA pepA* (G676T)	This study
S6	*lacZ sm*^{R} *toxT*::*lacZ ctxA nqr nhaA pepA* (G676T)	This study
S7	*lacZ sm*^{R} *toxT*::*lacZ ctxA nqr nhaA* P_{nhaB} (G-189A)	This study
S8	*lacZ sm*^{R} *toxT*::*lacZ ctxA nqr nhaA pepA* (T470A)	This study
S9	*lacZ sm*^{R} *toxT*::*lacZ ctxA nqr nhaA* P_{pepA} (-162ΔT)	This study
S10	*lacZ sm*^{R} *toxT*::*lacZ ctxA nqr nhaA* P_{nhaB} (G-189A)	This study
S11	*lacZ sm*^{R} *toxT*::*lacZ ctxA nqr nhaA pepA* (G491T) *csrA* (A31C)	This study
S12	*lacZ sm*^{R} *toxT*::*lacZ ctxA nqr nhaA pepA* (G491T) *csrA* (A31C)	This study
S13	*lacZ sm*^{R} *toxT*::*lacZ ctxA nqr nhaA pepA* (G491T) *csrA* (A31C)	This study
S14	*lacZ sm*^{R} *toxT*::*lacZ ctxA nqr nhaA pepA* (C490A) P_{nhaB} (Δ-388 – -361 (ΔAATAAACTTACTCGAAAGAGGTATTTCT)) Δ71878-72267[c] (tRNA^{Arg} (VC0395_A0077) tRNA^{Ser} (VC0395_A0078) tRNA^{Arg} (VC0395_A0079))	This study
S15	*lacZ sm*^{R} *toxT*::*lacZ ctxA nqr nhaA pepA* (T482A) VC0395_A2444 (134ΔA) *motY* (C604A)	This study
S16	*lacZ sm*^{R} *toxT*::*lacZ ctxA nqr nhaA* P_{nhaB} (A-345G) *pilA* (G221A)	This study
S17	*lacZ sm*^{R} *toxT*::*lacZ ctxA nqr nhaA* P_{nhaB} (A-345G)	This study
S18	*lacZ sm*^{R} *toxT*::*lacZ ctxA nqr nhaA* P_{nhaB} (A-12G) *secA* (Δ2233 – 2262 (ΔGAGGTTTATAAAGCCAAAGAGCAAGCGGTT)) VC0395_0946 (1013_1014 ins ACCAGA)	This study
S19	*lacZ sm*^{R} *toxT*::*lacZ ctxA nqr nhaA* P_{nhaB} (A-12G) *spoT* (C1176A)	This study
S20	*lacZ sm*^{R} *toxT*::*lacZ ctxA nqr nhaA* P_{nhaB} (A-12G) *rpoB* (C2623T) VC0395_0028 (C498T)	This study

[a]Recognition sites of restriction enzymes are underlined. [b]The identified mutations are specified in relation to the start codon of the indicated genes. [c]The numbers indicate the chromosome coordinates.